Tectonic implications of new Late Cretaceous paleomagnetic constraints from Eastern Liaoning Peninsula, NE China.

Wei Lin, Yan Chen, Michel Faure, Qingchen Wang

JOURNAL OF GEOPHYSICAL RESEARCH, VOL. 108, NO. B6, 2313, doi:10.1029/2002JB002169, 2003

Tectonic implications of new Late Cretaceous paleomagnetic constraints from Eastern Liaoning Peninsula, NE China

Wei Lin[1]
Institute of Geology and Geophysics, Chinese Academy of Sciences, Beijing, China

Yan Chen and Michel Faure
Département des Sciences de la Terre, Institut des Sciences de la Terre d'Orléans, Université d'Orléans, Orléans, France

Qingchen Wang
Institute of Geology and Geophysics, Chinese Academy of Sciences, Beijing, China

Received 31 December 2002; revised 11 February 2003; accepted 6 March 2003; published 21 June 2003.

[1] A paleomagnetic study has been carried out in the east of the Tan-Lu fault, in Liaoning Province, NE China, to understand the timing of Tan-Lu fault activity. Samples aging from Early Paleozoic to Late Mesozoic from 51 sites have been analyzed. Paleozoic and Late Permian-Early Triassic rocks are remagnetized by the recent geomagnetic field; however, Late Cretaceous (between 118 and 83 Ma) red tuffaceous sandstone passes a positive fold test, shows no Present Earth Field characteristic remanent magnetization carried by both magnetite and hematite, presents a solo normal polarity, and thus provides the only reliable paleomagnetic data in this study. The paleomagnetic pole calculated from these rocks (λ_p = 59.4°N, ϕ_p = 205.5°E, and A_{95} = 7.3°) is statistically undistinguishable from all available Cretaceous paleomagnetic data from Eastern Liaoning-Korean Peninsula, indicating that these areas may belong to a single tectonic unit, here named the East Liaoning-Korea (ELK) Block, at least since the Late Cretaceous. Conversely, a significant discrepancy between the ELK Block and Chinese Block (i.e., North and South China Blocks) characterized by a differential rotation (22.5° ± 10.2°) with a negligible latitudinal displacement (0.8° ± 6.1°) is demonstrated. This result indicates, first, that the left-lateral displacement along the Tan-Lu fault, if any, must have occurred before the Late Cretaceous and, second, that the Korean Block can not be considered as a rigid part of North China Block. Sedimentological and structural evidence show that the Meso-Cenozoic triangle shaped plain, consisting of Songliao, Xialiaohe, Sanjiang, Zeya, and other smaller basins developing in northeast China and southeast Russia, south of the Mongol-Okhotsk Belt, experienced a heterogeneous rifting from the Late Jurassic to Tertiary. The variable amount of extension, larger in the northeast (~300 km) than in the southwest (~80 km), is probably related to the clockwise rotation of the ELK Block centered at the south of the Bohai Bay Basin. This result shows that a significant segment of the East Eurasian margin (more than 1000 km long) experienced differential rotation in Cenozoic times. *INDEX TERMS:* 1518 Geomagnetism and Paleomagnetism: Magnetic fabrics and anisotropy; 1525 Geomagnetism and Paleomagnetism: Paleomagnetism applied to tectonics (regional, global); 1527 Geomagnetism and Paleomagnetism: Paleomagnetism applied to geologic processes; 8105 Tectonophysics: Continental margins and sedimentary basins (1212); 8157 Tectonophysics: Plate motions—past (3040); *KEYWORDS:* paleomagnetism, rifting, continental margin Meso-Cenozoic geodynamics, Songliao Basin, northeastern China plain

Citation: Lin, W., Y. Chen, M. Faure, and Q. Wang, Tectonic implications of new Late Cretaceous paleomagnetic constraints from Eastern Liaoning Peninsula, NE China, *J. Geophys. Res.*, *108*(B6), 2313, doi:10.1029/2002JB002169, 2003.

1. Introduction

[2] The main part of China landmass was formed by the welding of North China Block (NCB) and South China Block (SCB) as argued from geologic evidence [e.g., *Mattauer et al.*, 1985; *Sun et al.*, 1991; *Okay et al.*, 1993; *Xu et al.*, 1994], geochronology [e.g., *Li et al.*, 1993], metamorphic history [e.g., *Cong*, 1996], and paleomagnetic investigations [e.g., *Zhao and Coe*, 1987; *Enkin et al.*, 1992; *Gilder and*

[1]Now at Department of Earth and Planetary Sciences, Graduate School of Science, Nagoya University, Nagoya, Japan.

0148-0227/03/2002JB002169$09.00

Courtillot, 1997]. However, the intracontinental deformation continues at different scales in Mesozoic and Cenozoic times [e.g., *Chen*, 1998]. Some phenomena such as the intrusion of numerous Cretaceous granitic plutons in southeast China [e.g., *Jahn et al.*, 1990] or the eastward extrusion of south China along the Qinling fault due to India-Eurasia collision [e.g., *Peltzer et al.*, 1985; *Avouac and Tapponnier*, 1993] are well documented. Moreover, some processes such as the evolution of the Tan-Lu fault are still hotly debated. On the basis of geologic correlation on the both sides of the fault, a left-lateral displacement of several hundred kilometers from the Late Jurassic to Early Cretaceous has been proposed [*Xu et al.*, 1987]. Paleomagnetic results from the Shandong and Anhui Provinces do not support any relative motion since the Late Cretaceous [e.g., *Gilder et al.*, 1999], this result complies with geological observations showing that during the Late Cretaceous the Tan-Lu fault was a brittle normal fault [e.g., *Mattauer et al.*, 1985; *Faure et al.*, 1999; *Ratsbacher et al.*, 2000]. Moreover, a paleomagnetic study from the Liaoning Province and South Korea, i.e., east of the Tan-Lu fault, suggests a left-lateral motion of nearly 800 km along the fault since the Late Cretaceous [*Uchimura et al.*, 1996; *Uno*, 2000]. In order to clarify these confusions a paleomagnetic study has been carried out in the Liaoning Province, NE China, from the Early Paleozoic to Late Mesozoic periods.

2. Geological Setting and Paleomagnetic Sampling

2.1. Geological Outline

[3] In eastern Asia, several continental blocks, namely, from north to south, Siberia, Mongolia, north China, and south China separated by orogenic belts and suture zones of Mongol-Okhotsk, Xing-Meng, and Qinling-Dabie, respectively, are well acknowledged (Figure 1). Other sutures (e.g., Amur suture in Sikhote Alin or in Japan) are interpreted as marks of microcontinent collisions [e.g., *Faure and Natal'in*, 1992; *Natal'in*, 1993; *Ren et al.*, 2002, and references therein]. Moreover, those ancient plate boundaries are cut at high angle by major faults such as Tan-Lu and its northern continuations in the Yilan-Yiton and Fushun-Mishan faults or the Shikhote Alin fault (Figure 1). In NE China, the Liaoning Province, geographically situated near the border with North Korea, is considered as the easternmost part of the North China Block [*Bureau of Geology and Mineral Resources of Liaoning Province* (BGMRLP), 1989; *Bureau of Geology and Mineral Exploration and Development of Liaoning Province* (BGMEDLP), 1997, and references therein). There an Archean and Paleoproterozoic basement is overlain by a well-developed Neoproterozoic-Paleozoic-Early Mesozoic sedimentary cover. This lithostratigraphic pile is intruded by numerous Mesozoic granitic plutons and overlain by mainly continental Cretaceous-Tertiary basins filled by terrigenous and volcano-clastic deposits and intercalated by lava flows.

2.2. General Stratigraphy and Sedimentology of the Sampling Area

[4] In Liaoning Province, outcrops are generally well exposed with rock ages spanning from the Mesoproterozoic to Early Cenozoic [*BGMEDLP*, 1997]. Above the Archean metamorphic basement, the Paleoproterozoic series consists of weakly metamorphosed (i.e., greenschist facies) rocks, dominantly volcanic rocks and Mg-rich detrital ones in the lower and upper parts, respectively. The Neoproterozoic series (sampled Qingbaikou group) is characterized by sediments of shallow marine environment. In the sampling area the rocks have experienced a low-grade (prehnite-pumpelyite facies) metamorphism with a stratigraphic thickness <100 m. The Early Paleozoic strata are also shallow marine sediments, and their lithology is essentially platform limestone. The thickness of this series varies from 1200 to 2600 m. Abundant characteristic fossils, such as trilobite, graptolite, cephalopoda, and conodont, are used to constrain the stratigraphic age. The Late Paleozoic series is marked by alternation of continental and shallow marine sedimentary facies. Typical fossils are of brachiopoda, corals, foraminifera, and plants. In the study area the Mesozoic and Cenozoic periods correspond to the time of an important development of continental rifting basins with a sedimentary thickness over >10 km.

2.3. Sedimentology of Sampling Sites

[5] Table 1 and Figure 2 show the paleomagnetic sites collected from this study. Three main age groups are distinguished, namely, (1) Paleozoic (essentially Middle Ordovician and Middle-Upper Carboniferous) limestone-sandstone and (2) Upper Permian to Lower Triassic coarse red sandstone (P_2-Tr_{1s}) and Late Cretaceous red tuffaceous sandstone (K_{2d}).

2.3.1. Paleozoic Rocks

[6] In the Paleozoic rock group, three subgroups are differentiated on the basis of age and lithology: the Majiagou group of Middle Ordovician limestone (O_{2m}), the Benxi group of Middle Carboniferous sandstone (C_{2b}), and the Taiyuan group of Late Carboniferous limestone (C_{3t}).

[7] The Middle Ordovician age of the Majiagou group is defined by trilobite (*Pseudouphus*), cephalopoda (*Stereoplasmoceras, Polydesmia, Orodosoceras, Wutinoceras and pseudoseptatum*), and conodont (*Erticodon tangshanensis*). This O_{2m} stratum is essentially composed of thick limestone intercalated by dolomite. This group is in conformity with the underlying Lower Ordovician Liangjiashan group (O_{1l}) and in parallel or weakly angular unconformity with the overlying Middle Carboniferous Benxi group (C_{2b}). The total thickness of the Majiagou group is $\sim$300–500 m in the sampling area. Eighteen sites are taken from this formation with variable bedding directions (Table 1 and Figures 2b and 2c).

[8] The Benxi group of the Middle Carboniferous (C_{2b}) age consists mainly of continental facies thick yellow-green-gray coarse sandstone or micro conglomerate intercalated with shale and coal beds. The thickness of a single layer may reach 30 m. Numerous fossils have been identified in this formation, such as plants (*Sublepidodendron mirabile, Neuropteris gigantea*), Brachiopoda (*Linoproductus sp., Burtunia cf. Juresanensis*). In the research area this 300-m-thick series, in which four sites are collected (Table 1), is conformably overlain by the Taiyuan group.

[9] The Upper Carboniferous Taiyuan group (C_{3t}) lithologically belongs to marine and continental alternations of limestone intercalated by sandstone. Its thickness is variable from 60 to 230 m, and characteristic foramminifera fossils such as *Profusulinella*, *Eostaffela* are used to date this stratum. This series is in conformity with overlying and underlying neighboring strata. Eleven sites are drilled

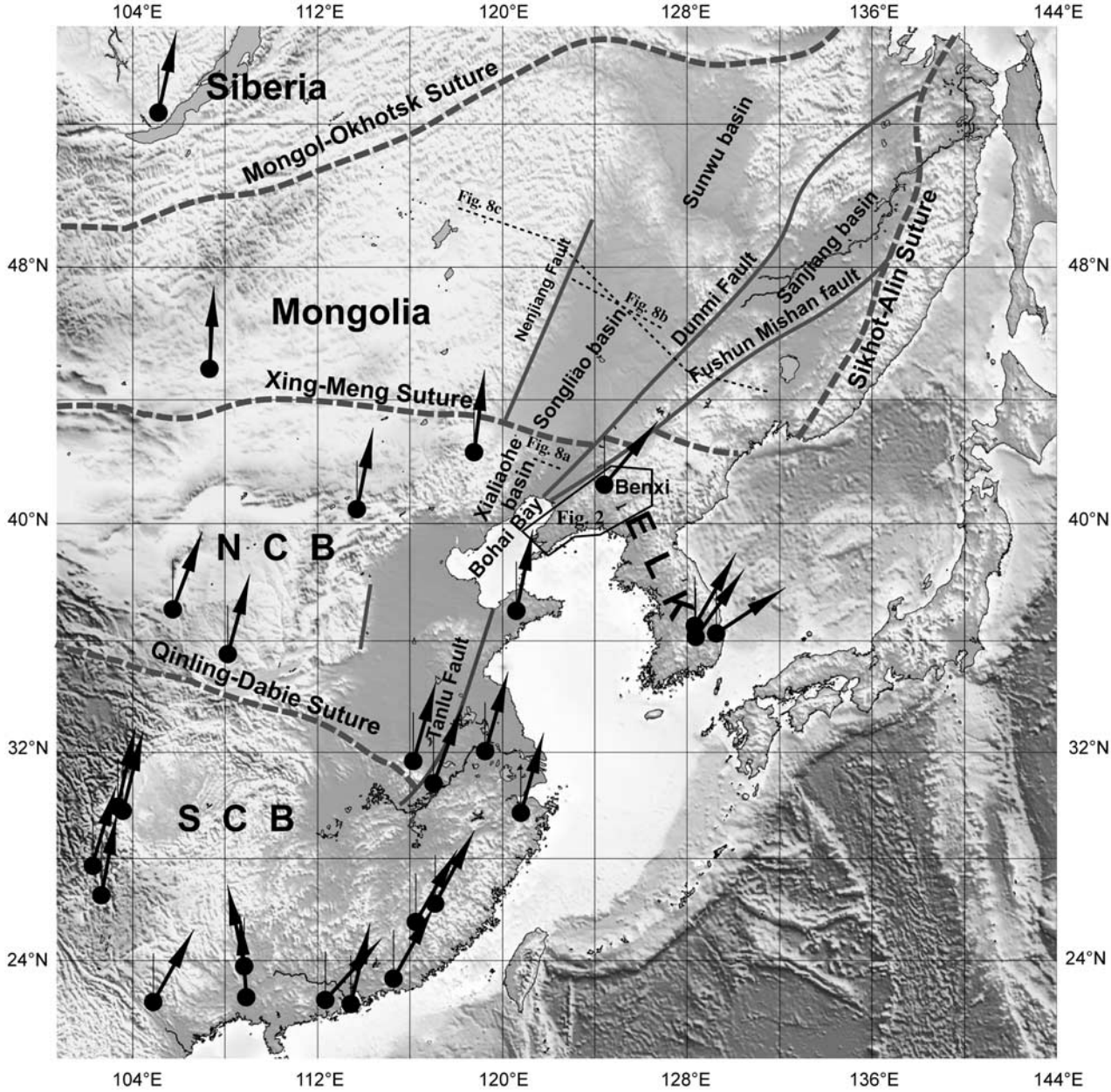

Figure 1. Topographic map of East Asia with simplified tectonic sketch. NCB, SCB, and ELK stand for North China Block, South China Block, and Eastern Liaoning-Korea Block, respectively. The arrows are the Cretaceous magnetic declinations of East Asia calculated from the data listed in Table 3 at the geographic site of Benxi (41.3°N, 123.84°E).

from the Late Carboniferous Taiyuan group (Table 1 and Figures 2b and 2c).

2.3.2. P_2-Tr_1 Shiqianfeng Group

[10] This group, of continental arid endoreic fluvial-lacustrine facies, is composed of dark red coarse-grained to conglomeratic sandstone with well-developed cleavage. It is conformably underlain by the Lower Permian Shihezi group and overlain by the Lower Triassic Linjia group with an angular contact. The thickness may reach to ~900 m. Some plants and bivalve fossils have been described for this formation, such as *Gigantonodechallai nicotianaefolia, Lobatannularia heianensis*. The bedding of this formation exposed in the western side of Benxi city varies very slightly; therefore the five sampled sites will not offer a fold test (Table 1 and Figure 2b).

2.3.3. Late Cretaceous Dayu Group (K_{2d})

[11] This group consists of dark red to violet colored fine tuffaceous sandstone in the lower part and dark red to gray muddy sandstone on the top. The total thickness exceeds 1200 m. Few plant-type fossils are found in this formation, such as *Frenelopsis*. The age determination depends mainly on the stratigraphic relationship with the underlying formation and facies correlation with similar rocks. The Dayu group is unconformably underlain by the Xiaoling group. The age for the Xiaoling group is still in debate. A Late Jurassic-Early Cretaceous age was attrib-

Table 1. Paleomagnetic Sampling in Eastern Liaoning[a]

Site	Geographic Coordinates Latitude, Longitude	*N*	Rock	Age	Formation	Bedding Strike	Bedding Dip
1	41°23′11.7″N, 123°57′48.4″E	7	muddy limestone	Qn_q	Qingbaikou	177.0	34.1
2	41°23′11.7″N, 123°57′48.4″E	7	muddy limestone	Qn_q	Qingbaikou	172.3	38
3	41°20′53.1″N, 123°53′57.6″E	7	yellow sandstone	P_{1s}	Shihezi	249.9	31.6
4	41°20′53.1″N, 123°53′57.6″E	8	yellow sandstone	P_{1s}	Shihezi	217.1	15.6
5	41°20′53.1″N, 123°53′57.6″E	9	yellow sandstone	P_{1s}	Shihezi	234.2	24.8
6	41°20′28.4″N, 123°54′18.7″E	6	microconglomerate	$C\text{-}P_s$	Shanxi	242.7	22.5
7	41°17′17.7″N, 123°43′20.1″E	6	coarse red sandstone	$P_2\text{-}Tr_{1s}$	Shiqianfeng	95.7	11.0
8	41°17′17.7″N, 123°43′20.1″E	6	coarse red sandstone	$P_2\text{-}Tr_{1s}$	Shiqianfeng	86.8	15.5
9	41°17′17.7″N, 123°43′20.1″E	6	coarse red sandstone	$P_2\text{-}Tr_{1s}$	Shiqianfeng	106.0	16.0
10	41°17′17.7″N, 123°43′20.1″E	6	coarse red sandstone	$P_2\text{-}Tr_{1s}$	Shiqianfeng	87.7	24.0
11	41°17′17.7″N, 123°43′20.1″E	6	coarse red sandstone	$P_2\text{-}Tr_{1s}$	Shiqianfeng	95.7	14.5
12	41°20′38.8″N, 123°43′12.5″E	6	limestone	O_{2m}	Majiagou	151.7	16.5
13	41°20′38.8″N, 123°43′12.5″E	6	limestone	O_{2m}	Majiagou	148.7	21.0
14	41°20′38.8″N, 123°43′12.5″E	7	limestone	O_{2m}	Majiagou	156.7	24.5
15	41°20′09.4″N, 123°42′50.3″E	7	yellow sandstone	C_{2b}	Benxi	133.7	28.5
16	41°20′09.4″N, 123°42′50.3″E	6	yellow sandstone	C_{2b}	Benxi	115.2	19.5
17	41°20′59.0″N, 123°42′28.6″E	5	brown sandstone	C_{2b}	Benxi	266.7	37.0
18	41°21′06.0″N, 123°42′43.9″E	6	limestone	O_{2m}	Majiagou	111.7	44.0
19	41°21′11.1″N, 123°42′55.5″E	6	limestone	O_{2m}	Majiagou	133.4	34.0
20	41°21′11.1″N, 123°42′55.5″E	6	limestone	O_{2m}	Majiagou	132.7	32.0
21	41°21′52.8″N, 123°42′48.1″E	5	limestone	O_{2m}	Majiagou	124.4	30.8
22	41°21′02.2″N, 123°50′10.1″E	7	limestone	O_{2m}	Majiagou	349.4	25.0
23	41°21′02.2″N, 123°50′10.1″E	6	limestone	O_{2m}	Majiagou	6.0	24.0
24	41°24′41.6″N, 123°52′08.8″E	7	red shale and sandstone	C_{3t}	Taiyuan	66.1	42.8
25	41°24′41.6″N, 123°52′08.8″E	7	gray-white sandstone	C_{3t}	Taiyuan	109.7	21.0
26	41°24′08.4″N, 123°52′08.4″E	7	yellow-brown sandstone	C_{3t}	Taiyuan	146.7 ~ 182.3	21 ~ 17
27	41°24′08.4″N, 123°52′08.4″E	7	yellow-brown sandstone	C_{3t}	Taiyuan	182.3	22.0
28	41°20′54.9″N, 123°55′56.0″E	5	yellow sandstone	C_{2b}	Benxi	127.0	42.2
29	41°18′17.7″N, 123°48′16.0″E	5	red tuffaceous sandstone	K_{2d}	Dayu	344.9	29.6
30	41°18′17.7″N, 123°48′16.0″E	5	red tuffaceous sandstone	K_{2d}	Dayu	15.7	13.5
31	41°18′17.7″N, 123°48′16.0″E	8	red tuffaceous sandstone	K_{2d}	Dayu	296.7	22.0
32	41°18′17.7″N, 123°48′16.0″E	5	red tuffaceous sandstone	K_{2d}	Dayu	16.7	22.0
33	41°18′17.7″N, 123°48′16.0″E	6	red tuffaceous sandstone	K_{2d}	Dayu	307.7	19.0
34	41°18′17.7″N, 123°48′16.0″E	7	red tuffaceous sandstone	K_{2d}	Dayu	303. 7	18.0
35	41°18′17.7″N, 123°48′16.0″E	5	red tuffaceous sandstone	K_{2d}	Dayu	312.7	19.0
36	39°24′28.4″N, 121°39′39.7″E	6	yellow-green sandstone	C_{3t}	Taiyuan	197.0	8.0
37	39°24′28.4″N, 121°39′39.7″E	8	yellow-green sandstone	C_{3t}	Taiyuan	193.7	9.0
38	39°24′28.4″N, 121°39′39.7″E	7	yellow-green sandstone	C_{3t}	Taiyuan	193.7	6.0
39	39°22′37.3″N, 121°40′13.1″E	6	limestone	O_{2m}	Majiagou	302.1	30.8
40	39°22′37.3″N, 121°40′13.1″E	6	limestone	O_{2m}	Majiagou	333.7	23.0
41	39°22′37.3″N, 121°40′13.1″E	6	limestone	O_{2m}	Majiagou	319.2	25.5
42	39°22′37.3″N, 121°40′13.1″E	6	limestone	O_{2m}	Majiagou	297.2	19.0
43	39°22′37.3″N, 121°40′13.1″E	6	limestone	O_{2m}	Majiagou	309.2	20.4
44	39°24′32.0″N, 121°39′50″.0E	6	yellow-green sandstone	C_{3t}	Taiyuan	321.4	27.8
45	39°10′20.4″N, 121°40′02.0″E	5	limestone	C_{3t}	Taiyuan	225.5	40.5
46	39°10′20.4″N, 121°40′02.0″E	6	limestone	C_{3t}	Taiyuan	207.7	42.0
47	39°10′20.4″N, 121°40′02.0″E	5	limestone	C_{3t}	Taiyuan	228.7	52.3
48	39°09′46.5″N, 121°39′54.5″E	7	limestone	O_{2m}	Majiagou	46.4	46.3
49	39°09′46.5″N, 121°39′54.5″E	6	limestone	O_{2m}	Majiagou	50.2	58.9
51	39°11′24.3″N, 121°35′18.9″E	6	limestone	O_{2m}	Majiagou	165.2	39.0
52	39°11′24.3″N, 121°35′18.9″E	5	limestone	O_{2m}	Majiagou	155.7 ~ 74	42 ~ 20

[a]Latitude and longitude are present latitude and longitude of sampling site. *N*, number of sampled cores from the corresponding site.

uted to this formation [*Zheng and Zhang*, 1981; *BGMRLP*, 1989]. On the top, the Dayu group is unconformably overlain by Quaternary conglomerates. On the basis of the fossil composition, *BGMEDLP* [1997] proposed that these red beds of the Dayu group belong to the lower part of Upper Cretaceous. Seven sites are collected in the northern part of Benxi city with variable bedding orientations (Table 1 and Figure 2b).

[12] Paleomagnetic sampling was carried out with a gasoline powered drill. Five to eight cores were taken in each site presenting a stratigraphic thickness of 5–10 m. Both magnetic and Sun compasses, when it was possible, were used for the core orientation. The average of difference between these two azimuths is about 8.3° ± 3.3°, and this value is applied to the correction for the cores that do not possess solar measurements as well as bedding strikes.

3. Paleomagnetic Results

3.1. Laboratory Measurement and Directional Analytic Techniques

[13] In the laboratory, cores are prepared into standard specimens with 2.5 cm in diameter and 2.2 cm in length. Thermomagnetic experience is carried out by KLY3 kappa-bridge coupled with CS3 furnace. Magnetic hysteresis curves are obtained by a magnetic inductometer at Paleomagnetic Laboratory of Saint Maur (Paris), the anisotropy of magnetic susceptibility (AMS) was measured by KLY3

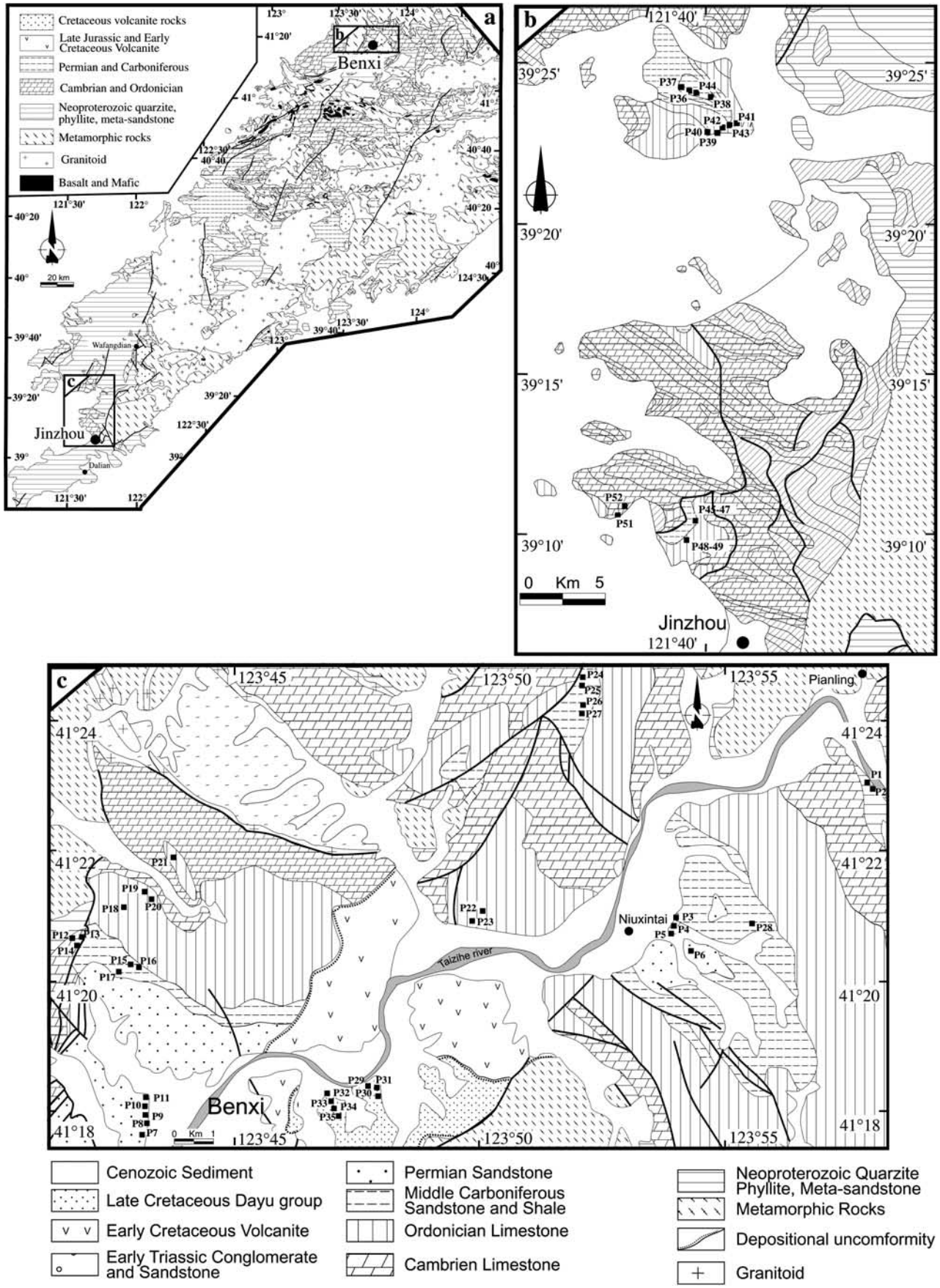

Figure 2. Simplified geological and paleomagnetic sampling maps of (a) Liaoning Province, (b) Benxi, and (c) Jinzhou areas, respectively. Solid squares represent sampling sites.

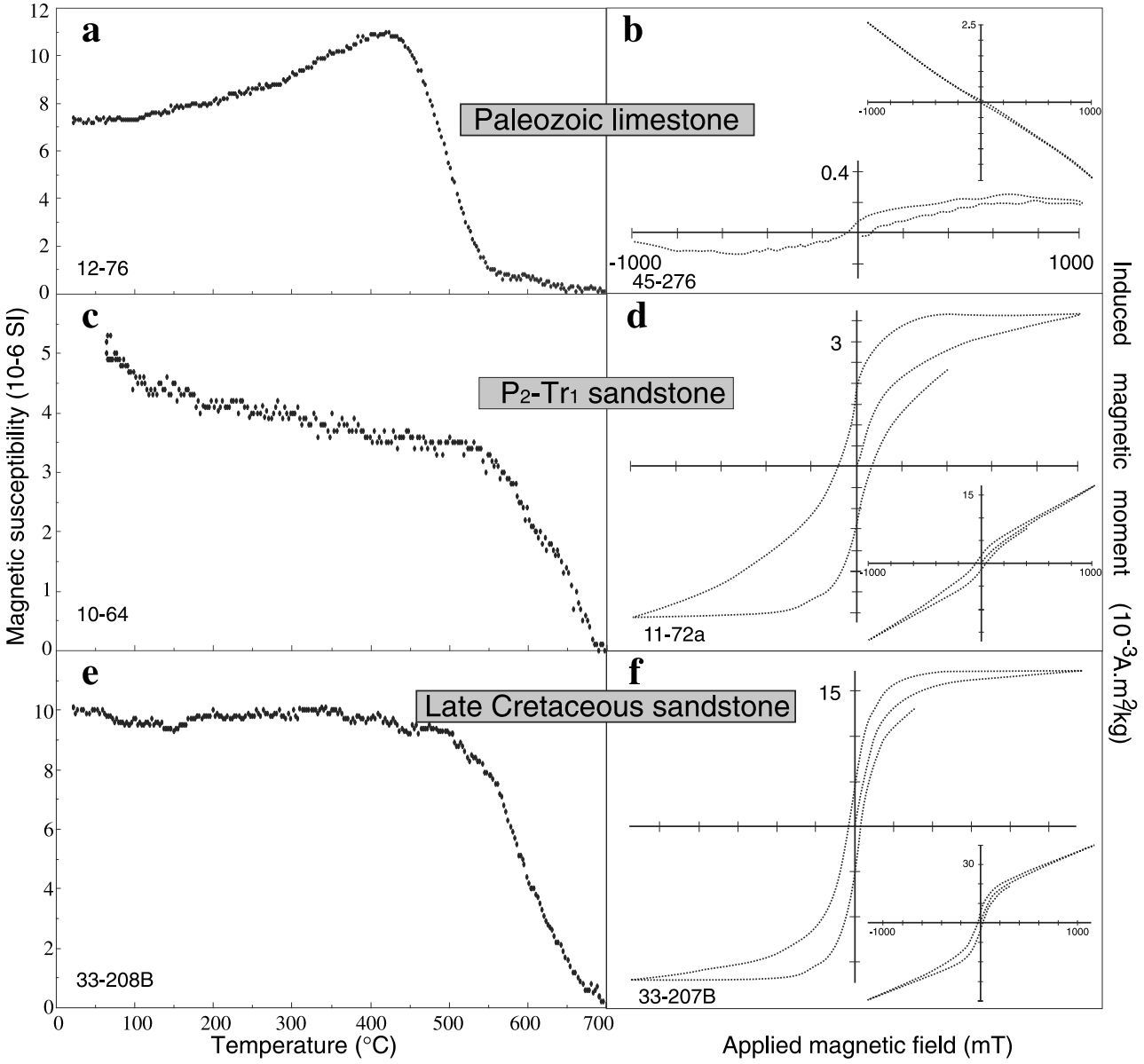

Figure 3. Magnetic mineralogical measurements. (a), (c), and (e) Thermomagnetic experiences and (b), (d), and (f) magnetic hysteresis curves for three age groups. The larger (smaller) curves show diamagnetic or paramagnetic reduced (bulk) measurements, respectively.

kappabridge. All sandstone and most limestone are subjected to progressive thermal and alternative filed (AF) demagnetizations by about 12 to 16 steps with temperature intervals from 200°C to 10°C and 2 to 20 mT, respectively. The magnetic remanence is measured by JR5 magnetometer at the Laboratoire de Magnétisme des Roches d'Orléans for all sandstone and by 2G cryogenic magnetometers at the Institut de Physique du Globe de Paris for partial limestone. Magnetic directions are isolated by the principal component analysis [*Kirschvink*, 1980] and mean magnetic directions are calculated by the spherical analysis [*Fisher*, 1953]. *Watson and Enkin* [1993] method is applied to fold test.

[14] Because the number of sites for some geologic periods, such as the Neoproterozoic Qingbaikou group (two sites) and the Carboniferous-Permian Shanxi group (one site), is too small to provide reliable paleomagnetic data, we present the results from 45 out of 51 sites for three main geologic periods: limestone-sandstone of the Paleozoic including O_{2m}, C_{2b}, C_{3t}, coarse red sandstone of the P_2-Tr_{1s} and tufaceous red sandstone of K_{2d}.

3.2. Paleozoic Limestone and Sandstone

[15] A generally weak natural remanent magnetization (NRM) was observed with a mean intensity of $1.24 \pm 0.9 \times 10^{-3}$ A/m for all Paleozoic limestone and yellow-gray-green-white sandstone. Though thermal magnetic experience from limestone presents a relatively important susceptibility drop from 450°C to 550°C, indicating that the magnetite is probably the principal remanence carrier (Figure 3a), the magnetic hysteresis curve shows a diamagnetic mineral dominance for the limestone (Figure 3b).

More than 60 specimens are demagnetized in the pilot study by both thermal and AF methods. Few sandstone samples show stable magnetic remanence (Figure 4a), and all limestone ones display a solo normal polarity (Figures 4b and 4c). The mean direction of these samples is more clustered in the geographic coordinates than that in stratigraphic ones: $D_g = 5.5°$, $I_g = 60.7°$, $\kappa_g = 75.5$, and $\alpha_{95g} = 2.7°$; $D_s = 341.6°$, $I_s = 63.3°$, $\kappa_s = 6.0$ and $\alpha_{95s} = 10.5°$ (Figure 5a). The negative fold test is concluded [*Watson and Enkin*, 1993]. The mean direction in geographic coordinates is close to the Present Earth Field (PEF)(the dipolar direction, $D = 0°$ and $I = 58.9°$; the IGRF direction, $D = 351.8°$ and $I = 58.9°$; Figure 5a).

3.3. P_2-Tr_1 Coarse Red Sandstone

[16] The average of NRM intensity for these coarse red sandstones is $\sim 9.18 \pm 3.86 \times 10^{-3}$ A/m. The Curie temperature experience displays two possible susceptibility drops at from 480 to 580 and 600 to 680, respectively (Figure 3c). The magnetic hysteresis curves present the dominance of paramagnetic minerals with magnetic induced saturation at 3.6×10^{-3} A m^2/kg and magnetic coercive force at 32.3 mT (Figure 3d). Thus the hematite could be considered as the main remanence carrier with a weak proportion of magnetite. Most thermal demagnetization reveals only a single component ranging from 20°C to 680°C (Figure 4d). Only a few specimens present a well-isolated and no originward ''lower'' temperature component with a tendency of another component at higher temperature (Figures 4e and 4f). Because of the small number of specimens and weak magnetic remanent intensity, no stable and reliable directions would be isolated and computed from the latter component. Fisher statistics of directions isolated from single, and sometimes ''lower'' temperature, component gives a slight better cluster distribution of directions in geographic coordinates than those in stratigraphic one: $D_g = 359.9°$, $I_g = 66.4°$, $\kappa_g = 510.5$ and $\alpha_{95g} = 3.4°$; $D_s = 353.7°°$, $I_s = 82.4°$, $\kappa_s = 216.4$ and $\alpha_{95s} = 5.2°$ (Figure 5b and Table 2). The fold test is negative according to *Watson and Enkin* [1993] method and the in situ mean direction is close to PEF (Figure 5b).

3.4. K_{2d} Fine-Grained to Muddy Sandstone

[17] This age group of fine-grained to muddy sandstone presents a higher proportion of soft magnetic minerals with respect to two former groups with a higher NRM intensity of $38.8 \pm 13.2\ 10^{-3}$ A/m. Magnetic hysteresis curves confirm this observation with higher magnetic induced saturation at 17.1×10^{-3} A m^2/kg and magnetic coercive force at 14.9 mT (Figure 3f). Curie temperature determination shows a stable susceptibility until nearly 500°C and a continuous drop from about 500°C to 680°C (Figure 3e). The above observations indicate that both magnetite and hematite may be the main magnetic remanence carriers. Some specimens present both lower- and higher-temperature components varying from 20°C to 300°C and 300°C to 680°C, respectively (Figure 4g). The remaining shows just a single component (Figure 4h). Both of them are of normal polarity, i.e., northeastward declination and downward inclination. The lower-temperature component shows scattered directions probably due to the magnetic viscosity. The higher-temperature component is interpreted as characteristic remanent magnetization (ChRM). The ChRM presents a better clustered distribution of directions in stratigraphic coordinates ($D_s = 40.1°$, $I_s = 57.9°$, $\kappa_s = 70.1$, and $\alpha_{95s} = 7.3°$) than those in geographic ones ($D_g = 39.6°$, $I_g = 75.4°$, $\kappa_g = 42.5$, and $\alpha_{95g} = 9.4°$; Figure 5c), giving a positive fold test with a maximum grouping of directions at 83.7% unfolding (with statistic uncertainties ranging from 68.7 to 95.1 [*Watson and Enkin*, 1993]). Thus a paleomagnetic pole is calculated: $\lambda_p = 59.4°$N, $\phi_p = 205.5°$E and $A_{95} = 7.3°$ (Table 3).

4. Interpretation and Discussion

4.1. Evidence for Clockwise Rotation of the ELK Block

[18] Three age groups have been paleomagnetically analyzed: Paleozoic limestone/yellow-gray sandstone, Permo-Triassic coarse red sandstone, and Late Cretaceous fine-grained to muddy red tuffaceous sandstone. The former two show better clustered magnetic directions in geographic coordinates, being undistinguishable from PEF, than those in stratigraphic ones and indicating a remagnetization. The Paleozoic limestone is well fractured, folded, and, sometimes, overturned. The fractures are often filled with secondary mineral crystallizations. The brittle deformation likely enhances fluid circulations that may produce a chemical remagnetization. In order to characterize the sedimentary fabrics of the P_2/Tr_{1s} coarse red sandstone, a study of the anisotropy of magnetic susceptibility (AMS) has been carried out on the rocks. The AMS measurements show a good cluster of the vertical axes of foliation poles (K_3) with a scattered distribution of maximum and intermediate axes, K_1 and K_2, respectively (Figure 6a). The mean values for the shape parameter, T, about 0.4, and for the anisotropy degree, P', ~ 1.025, are typical of sedimentary origin (Figure 6a) [*Tarling and Hrouda*, 1993]. This AMS observation implies that the P_2/Tr_1 red sandstone did not experience a significant tectonic deformation; therefore the remagnetization of the P_2/Tr_1 rocks could be either of chemical and/or thermal origins. In the study area the important Mesozoic and Early Cenozoic thermal events have been evidenced in widespread zones but with few Quaternary ones mostly concentrated in the Changbaishan mountain at the boundary between China and North Korea [*Cheng*, 1990; *Liu*, 1988] and in the northern part of research area [*Liaoning Bureau of Geology and Mineral Resources-Kuandian*, 1967]. The isolated direction from this coarse red sandstone, being consistent with PEF, should be a record of the recent geomagnetic field for following reasons: (1) if the remagnetization age was older than the Late Cretaceous, these rocks should have suffered the same rotation as K_{2d} sandstone because of the geographic proximity between these two localities, and (2) the apparent polar wander path (APWP) of the Eurasian landmass predicts a significantly different paleoposition and a relatively rapid latitudinal drift of the studied area during the Tertiary [*Besse and Courtillot*, 2002]. Therefore the chemical origin of the remagnetization could be considered as main factor for these coarse red beds.

[19] The characteristic remanent magnetization (ChRM) of K_{2d} red tuffaceous sandstone carried by both magnetite and hematite and presenting a positive fold test probably

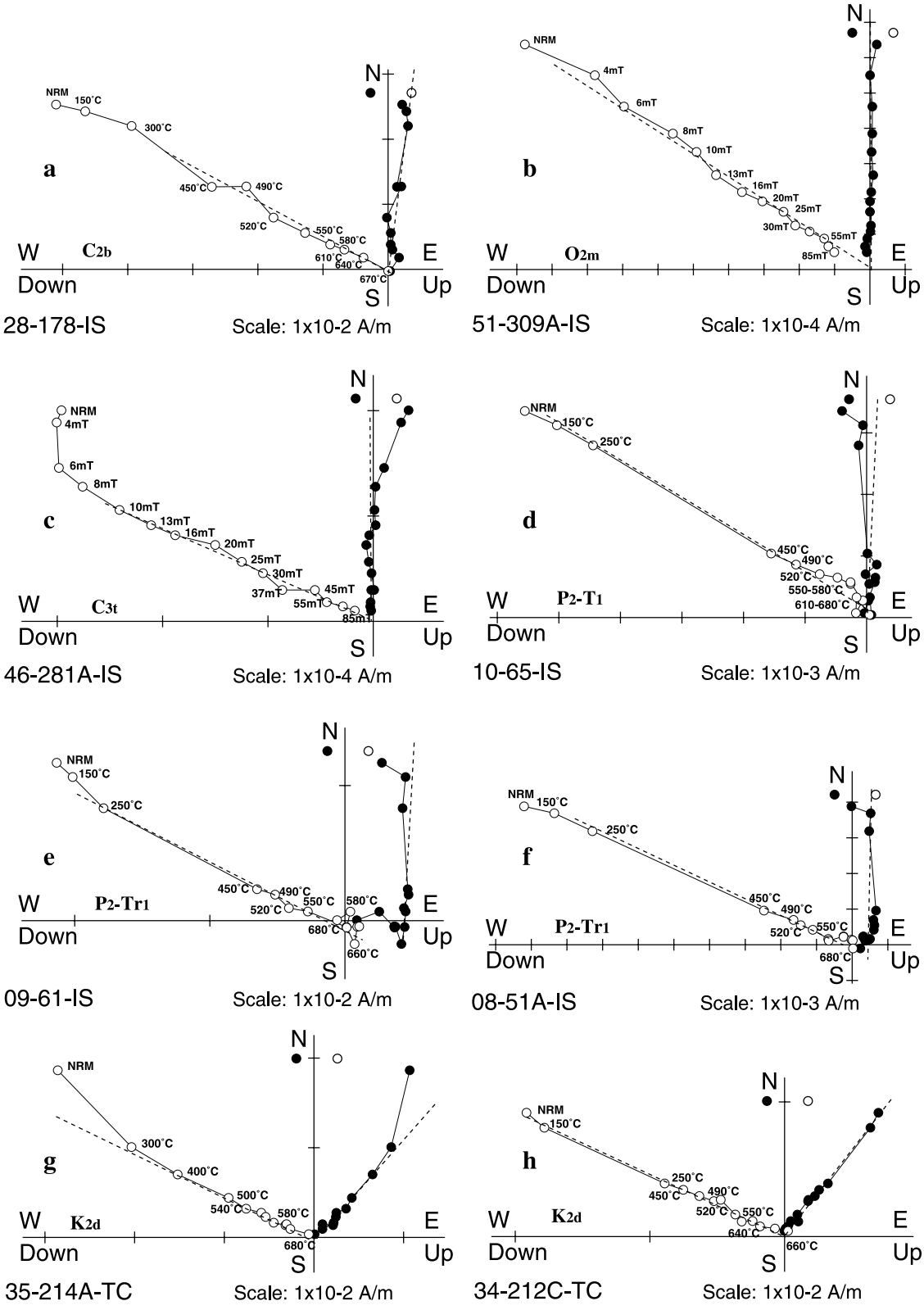

Figure 4. Representative orthogonal projections of magnetic directions from three age groups. Solids (circles) show the horizontal (vertical) plan. Dashed lines show the best fit directions. IS and TC stand for in situ (geographic) and tectonic corrected (stratigraphic) coordinates. Dashed lines show linear sector isolated for high-temperature component.

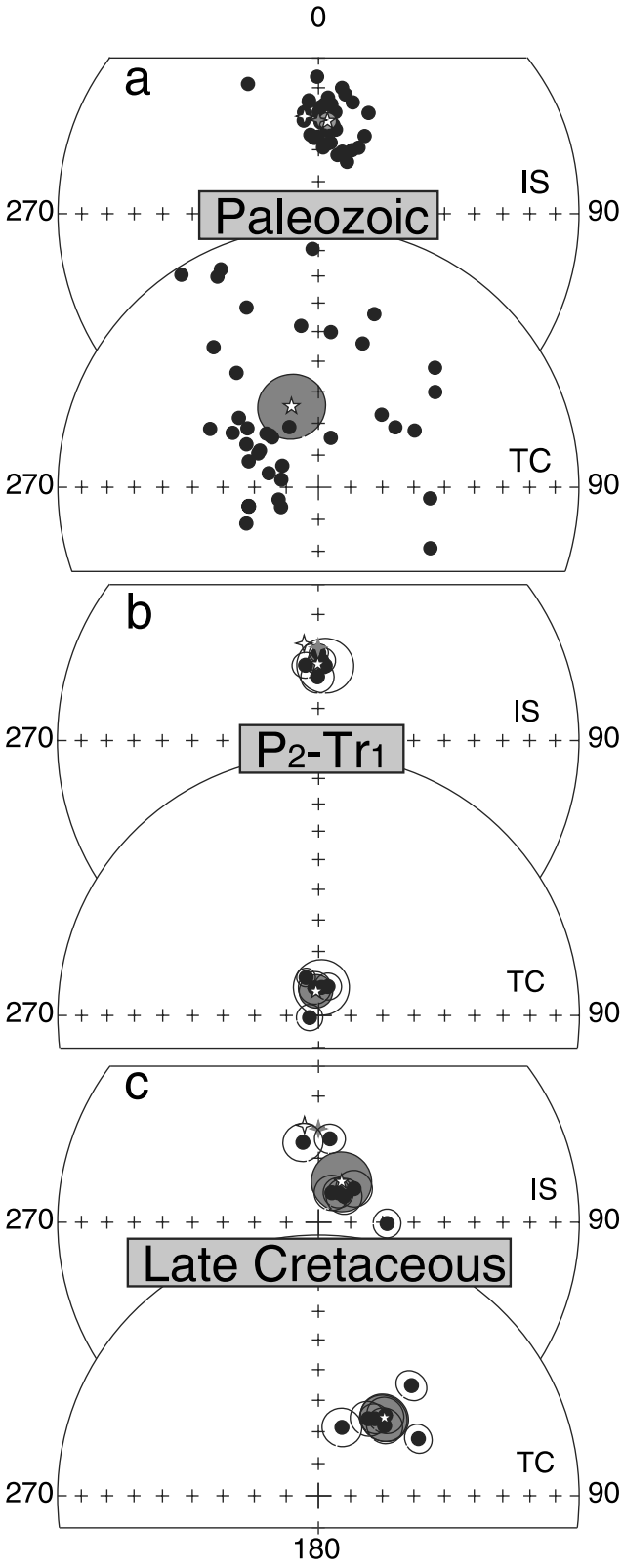

Figure 5. Equal-area projections of mean directions (a) at sample level for Paleozoic rocks and at site levels for (b) P_2-Tr_{1s} and (b) K_{2d} rocks. IS and TC stand for in situ (geographic) and tectonic corrected (stratigraphic) coordinates. Solid (open) diamond presents dipolar (actual) geomagnetic field of sampling areas. Star stands for the age mean direction.

Table 2. Paleomagnetic Results From P_2-Tr_{1s} and K_{2d} Age Groups[a]

		Geographic coordinates		Stratigraphic coordinates			
Site	*n*	D, deg	I, deg	D, deg	I, deg	κ	α_{95}, deg
P_2-Tr_{1s} Coarse Red Sandstone							
7	5	359.6	70.4	352.1	81.3	225.3	5.1
8	6	2.8	65.2	18.0	80.5	250.1	4.2
9	6	0.6	62.8	341.7	77.5	253.1	2.9
10	6	350.5	66.4	256.7	87.1	273.6	4.1
11	6	5.7	66.7	5.7	81.2	60.6	8.7
Mean[b]	5	359.9	66.4			510.5	3.4
Results[c]				353.7	82.4	216.4	5.2
K_{2d} Red Tuffaceous Sandstone							
29	5	7.8	63.5	40.2	43.8	270.5	4.7
30	3	349.0	64.4	19.0	67.3	409.7	6.1
31	8	24.4	79.9	32.9	61.1	103.1	5.5
32	5	91.0	68.5	60.3	53.5	304.9	4.4
33	6	33.8	78.9	36.2	59.9	207.8	4.7
34	5	46.6	74.7	39.8	56.9	179.8	5.7
35	5	44.5	78.6	43.4	59.6	190.5	5.6
Mean[b]	7	29.6	75.4			42.5	9.4
Results[c]				40.1	57.9	70.1	7.3

[a]*D*, *I*, κ, and α_{95} are magnetic declination, inclination, *Fisher* [1953] statistic precision parameter, and uncertainty at 95% confidence level, respectively.
[b]Statistical results before bedding correction.
[c]Statistical results after bedding correction.

shows a primary origin of magnetic remanence. Furthermore, the weak anisotropy degree of AMS (1.021) and the well-grouped but quasi-horizontal inclination of K_1 axes imply that these K_{2d} sandstones have not experienced important deformation since their diagenesis (Figure 6b). The solo normal polarity may indicate that the remanence age is comprised in the Cretaceous Long Normal Superchron (CLNS) between 118 and 83 Ma.

[20] More and more paleomagnetic data become available for both NCB and SCB, particularly for the Cretaceous age, with a relatively good geographic cover. Several paleomagnetic syntheses on their geodynamic history have been therefore proposed [e.g., *Enkin et al.*, 1992; *Gilder and Courtillot*, 1997; *Yang and Besse*, 2001]. One of their main conclusions is that these two continents did not experience a paleomagnetically observable relative displacement since the Early Cretaceous. This conclusion is illustrated in Figure 7b by all available Cretaceous poles from both NCB and SCB listed in Table 3. The angular difference computed from the polar averages of these two continents is statistically insignificant (3.2° ± 6.7°). Thus a mean paleomagnetic pole with λ_p = 77.7°N, ϕ_p = 205.9°E, and A_{95} = 3.7° (Table 3) can be calculated for the whole NCB and SCB (hereinafter this single landmass will be called "Chinese Block").

[21] On the basis of geological correlation on both sides of the Tan-Lu fault, *Xu et al.* [1987] argued for a relative left-lateral motion of several hundreds of kilometers along the Tan-Lu fault during the Late Triassic to Early Cretaceous period. Several models based on this large sinistral wrenching have been then proposed to account for the geodynamics of eastern Asia [e.g., *Kimura et al.*, 1990; *Yin and Nie*, 1993; *Xu and Zhu*, 1994; *Li*, 1994]. *Gilder et al.* [1999] published paleomagnetic results from Shandong and Anhui Provinces on the both sides of Tan-Lu fault with

Table 3. Available Cretaceous Paleomagnetic Poles From North China Block (NCB), South China Block (SCB), Eastern Liaoning-Korea Block (ELKB), and Eurasian Reference[a]

Age	Coordinates		N	λ_p	ϕ_p	A_{95}	References
	Lat, °N	Long, °E					
			North China Block (NCB)				
K_1	42.0	119.2	6	82.9	249.5	5.7	*Zhao et al.* [1990]
K_1	35.0	108.0	10	75.8	208.7	7.5	*Ma et al.* [1993]
K_1	37.0	120.7	11	81.3	217.3	5.9	*Gilder et al.* [1999]
K_1	45,4	107.6	3	87.3	247.6	21.6	*Pruner* [1992][b]
K_1	39.9	97.7	9	75.5	169.9	7.7	*Chen et al.* [2002]
Mean K_1			5	81.7	206.8	6.7	
K_{1-2}	37.2	105.0	10	74.5	203.4	8.2	*Wu et al.* [1993]
K_{1-2}	31.6	116.0	10	74.5	201.0	4.7	*Gilder and Courtillot* [1997]
K_2	40.1	112.9	4	79.6	170.1	5.8	*Zheng et al.* [1991]
Mean K_{1-2}			8	79.8	200.6	4.5	
			South China Block (SCB)				
K_1	29.7	120.3	7	77.1	227.6	5.5	*Lin* [1985]
K_1	22.2	114.2	12	78.2	171.9	10.6	*Chan* [1991]
K_1	30.0	102.9	23	77.9	244.5	3.2	*Enkin et al.* [1991]
K_1	25.9	101.7		64.6	199.6	3.3	*Otofuji et al.* [1998]
K_1	26.8	102.5	7	69.0	204.0	4.3	*Huang and Opdyke* [1992]
K_1	22.7	108.7	8	86.5	26.4	6.8	*Gilder et al.* [1993]
K_1	18.8	109.4	6	83.2	143.0	9.8	*Li et al.* [1995]
K_1	27.9	102.3	11s	77.4	196.2	14.5	*Zhu et al.* [1988]
Mean K_1			8	78.8	202.1	7.1	
K_2	25.0	116.4	20	67.9	186.2	9.2	*Hu et al.* [1990]
K_2	32.0	119.0	19	76.3	172.6	10.3	*Kent et al.* [1987]
K_2	23.0	115.0	43s	66.0	221.5	3.4	*Hsu* [1987]
K_2	26.0	117.2	5	66.9	221.4	5.4	*Zhai et al.* [1993]
K_2	30.8	117.5	4	83.8	200.2	14.6	*Gilder et al.* [1999][b]
K_2	30.0	102.9	16	74.8	250.8	6.6	*Enkin et al.* [1991]
K_2	26.5	102.3	18	81.9	220.9	7.1	*Huang and Opdyke* [1992]
K_2	26.0	117.3	20	65.1	207.2	5.0	*Gilder et al.* [1993]
K_2	23.1	113.3	19	56.2	211.5	3.9	*Gilder et al.* [1993]
K_2	23.7	108.7	9	79.4	7.1	10.0	*Gilder et al.* [1993]
K_2	26.6	102.4	20s	78.9	186.6	5.5	*Zhu et al.* [1988]
Mean K_2			11	75.2	210.7	7.5	
Mean K_{1-2}			19	76.7	207.6	5.0	
Mean K_{1-2}	NCB + SCB	27	77.7	205.9	3.7		
			Eastern Liaoning-Korean Block (ELKB)				
K_2	41.3	123.8	5	59.3	202.6	6.0	*Uchimura et al.* [1996]
K_2	41.3	123.8	7	59.4	205.5	7.3	this study
K	36.0	128.5	65	64.0	195.0	6.4/8.4	*Otofuji et al.* [1986]
K_1	35.9	128.5	19	67.6	205.1	5.8	*Lee et al.* [1987]
K_1	35.9	128.6	15	68.7	199.0	8.9	*Zhao et al.* [1999][b]
K_1	37.1	129.0	14	46.7	200.4	9.6	*Doh and Piper* [1994]
Mean K_{1-2}			6	61.0	201.3	6.8	
			Eurasia				
K 110 ± 10 Ma			18	79.9	181.9	3.9	*Besse and Courtillot* [2002]

[a]Lat and Long symbolize the geographic coordinates in latitude and longitude of corresponding study area; N (s) stands for the number of sites (samples); λ_p, ϕ_p and A_{95} present polar coordinates and uncertainty at 95% confidence level, respectively.
[b]Pole recalculated from original paper.

rock ages spanning from the Late Triassic to Early Cretaceous. The significant difference among the data older than Late Cretaceous from two sides of the fault and a good coherence among younger data led the authors to conclude that the relative motion along the fault, if there was any, should have occurred before the Late Cretaceous. If the Benxi area belonged to the Chinese Block at the age of the studied rocks (Figure 1), i.e., in the Late Cretaceous, this conclusion should also be sound for it. In other words, the Late Cretaceous paleomagnetic data from the Benxi area should be statistically consistent with those of the Chinese Block. However, the significant discrepancy of the Benxi area with Chinese Block by an angular difference of 18.5° ± 8.2° indicates that Benxi area has significantly moved with respect to the Chinese Block.

[22] To clarify if this relative motion corresponds either to a local one, as post-Cretaceous tectonics are not negligible in the study area, or to a continental-size block displacement, a review of previous paleomagnetic data from surrounding areas is necessary. In fact, a paleomagnetic study has been carried out on Paleozoic and Upper Cretaceous rocks near our sampling area [*Uchimura et al.*, 1996]. Though Uchimura et al. mentioned that the Paleozoic data are too scattered to give some tectonic explanation (probably due to remagnetization), the Upper Cretaceous paleomagnetic data are compatible to ours with an angular

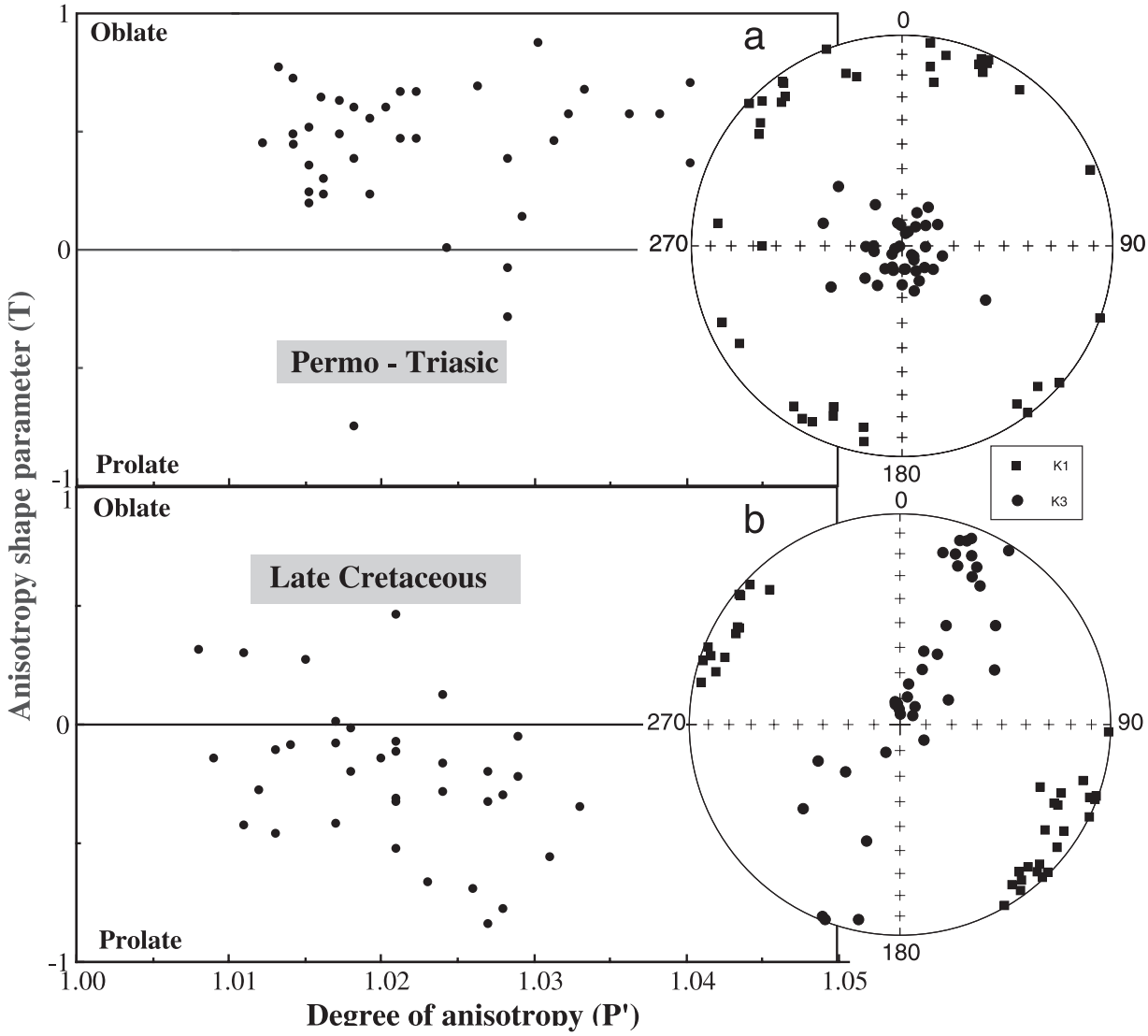

Figure 6. Anisotropy degree (P') against shape parameter (T) and equal-area projection of maximal (K_1) and minimal (K_3) axes of the anisotropy of magnetic susceptibility for P_2-Tr_{1s} and K_{2d} age groups. ($P = \exp\sqrt{\left[(\ln K_{max} - \ln K_{mean})^2 + (\ln K_{int} - \ln K_{mean})^2 + (\ln K_{min} - \ln K_{mean})^2\right]}$ with $K_{mean} = (K_{max} + K_{int} + K_{min})/3$; $T = [2 \ln (K_{int}/K_{min})/\ln(K_{max}/K_{min})] - 1$ [*Jelinek*, 1981]).

difference of 1.5° ± 9.4° (Table 3). *Zhao et al.* [1999] presented three apparent geomagnetic poles from the Taegu region (Ryongnam massif) in South Korea and argued that the Korean Peninsula has rotated clockwise by 34.3°, 24.9°, and −0.9° with respect to Eurasia during Early, Middle, and Late Aptian, respectively. As the uncertainty at 95% confidence level for the Cretaceous pole of the Eurasian reference is relatively small (3.9° [*Besse and Courtillot*, 1991]), the relative rotations are significant. However, if these three poles are projected in a same plot, their uncertainties overlap each other; in other words, they are not significantly different at 95% confidence limits. Moreover, because the Middle Aptian data resulted from three volcanic flows, it would be suspect whether the secular variation has been averaged out. If the relative rotations present a geological reality, a simple calculation of the possible rotation (35.2°) on the maximal Aptian duration (5 Ma [*Odin*, 1994]) gives an average rotation velocity of 7°/Myr, which seems too fast for this region as no important tectonic events have been documented for this period. On the basis of above reasons, we recalculate a mean pole from all sites of *Zhao et al.* [1999] (Table 3). Figure 7a presents all Cretaceous paleomagnetic data from different zones and types of rocks from East Liaoning and South Korea. Apart from that of *Otofuji et al.* [1986], the other five independent data are statistically consistent (Table 3). This observation leads us to suggest that Eastern Liaoning and Korea Peninsula may constitute a tectonically single and coherent unit, which is called the East Liaoning-Korea (ELK) Block in the following, at least since the Late Cretaceous. This paleomagnetic conclusion complies with geological evidence that in the Late Cretaceous the whole Korea Peninsula behaved as a unique continental mass. Therefore a mean pole for the ELK Block has been computed (Table 3).

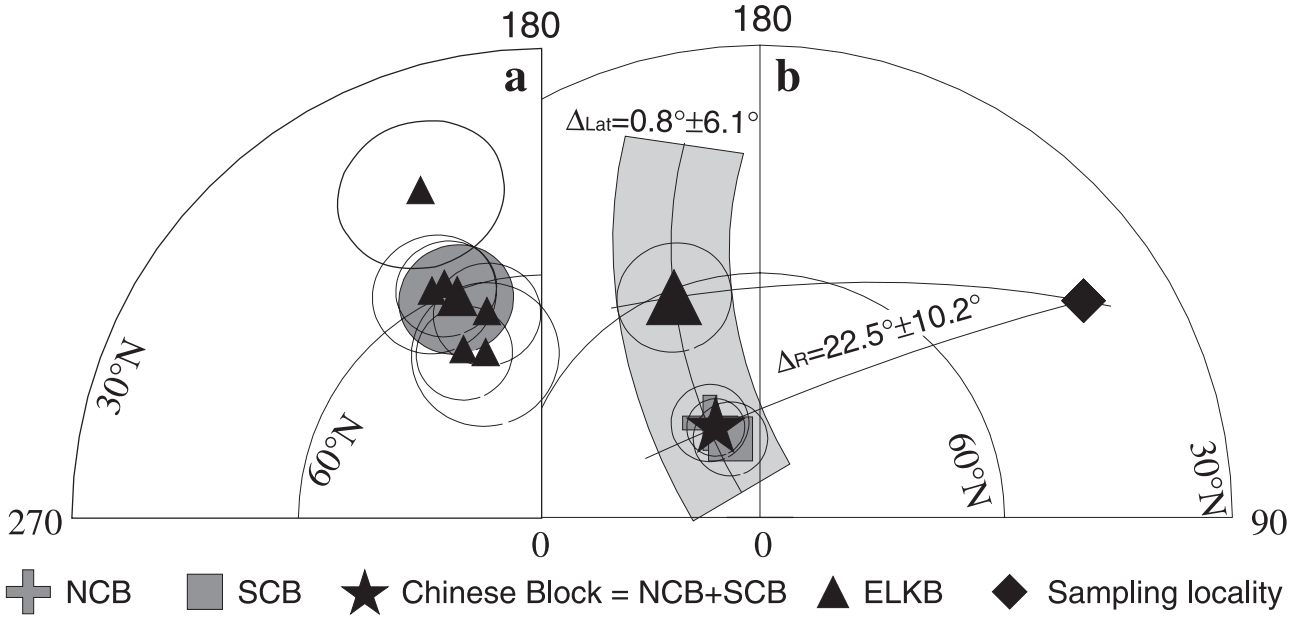

Figure 7. (a) All available magnetic poles from Eastern Liaoning and Korea Block (small triangles) with the corresponding average (large triangle). (b) Equal-area projection of mean paleomagnetic poles from NCB, SCB, and ELKB with the sampling locality of this study. Cross, square, star, triangle, and diamond show the mean poles from NCB, SCB, NCB + SCB, ELKB, and sampling locality, respectively. Δ_R and Δ_{Lat} show the relative difference in rotation and latitudinal displacement, respectively, between NCB + SCB and ELKB.

[23] The comparison of the ELK Block pole with that of the Chinese Block shows a statistically significant difference: 16.9° ± 7.6°. This angular difference presents a relative latitudinal motion of 0.8° ± 6.1° and a relative rotation of 22.5° ± 10.2° between these two tectonic units at the geographic reference of 41.3°N and 123.8°E (the sampling locality of this study). This calculation indicates that the relative motion between the ELK Block and the Chinese Block is essentially in the relative rotation instead of in the latitudinal displacement. In other words, the 800-km strike-slip motion along the northern continuity of Tan-Lu fault in Liaoning Province estimated by *Uchimura et al.* [1996] is not supported by our data. This conclusion is consistent with field observation. In several places in Jiangxi, Anhui, and Shandong Provinces, the Tan-Lu fault appears as a normal fault that controls the opening and sedimentary infill of Cretaceous continental red beds [e.g., *Mattauer et al.*, 1985; *Gilder et al.*, 1999; *Faure et al.*, 1999; *Ratsbacher et al.*, 2000; *Lin et al.*, 2000, also Polyphase deformation in the Feidong-Zhangbaling Massif (eastern China) and its place in the collision between North China and South China Blocks, submitted to *Tectonophysics*, 2002].

[24] Conversely to a classic tectonic explanation that would relate the clockwise rotation of ELK Block to the strike-slip motion along the Tan-Lu fault, we would like to propose here an alternative interpretation in which this discrepancy of paleomagnetic data between the Chinese and ELK Blocks is the result of the rifting of the Songliao and other basins of NE China.

4.2. Rifting of the NE China Basins

[25] The northeastern (NE) China plain consists of two major Meso-Cenozoic basins: the Xialiaohe and Songliao basins in the south and north, respectively (Figure 1). The Zeya basin in Russia is the northern continuation of the Songliao one, and other basins (Sanjiang, Boli, and Jixi) crop out east of the Yilan-Yitong fault (Figure 10a). It is worth noting, even from the topography, that this area which comprises the Meso-Cenozoic basins of NE China forms a triangular shape with a progressive width increase from the southwest to the northeast (Figure 1). A good understanding of the rifting history of these basins may bring new insights for the tectonic relationships between the ELK and Chinese Blocks.

[26] In the northern portion of the Bohai Bay basin, the Xialiaohe basin (Figure 1), started to rift in Paleocene and ended its extension in the Oligocene [*Yu*, 1989; *Allen et al.*, 1998]. The small amounts of Late Jurassic and Early Cretaceous volcanic rocks and coal-bearing sediments indicate an early but limited rifting episode (Figure 8a). The Songliao basin is a Late Mesozoic extensional basin (Figures 1 and 8b). The Late Jurassic fluvial and lacustrine sediments intercalated with volcanic rocks were preserved only in the deepest parts of the trough. The Early Cretaceous was the initial rifting period when the Denglouku formation (K_1) accumulated in 20 NNE trending grabens in which the fluvial and lacustrine sedimentary thickness is more than 2000 m (Figures 8b and 9). During Late Cretaceous, fluvial and lacustrine sediments more than 3000 m thick, corresponding to the Quantou to the Nenjiang formations (K_2), were deposited in a starved basin with an area of almost 7 times of that of previous grabens (Figure 8b). Numerous characteristic fossils, such as *Asterisporites radiata* and *A. stellate*, are frequently found in the upper portion of the Quantou formation. Angiospermous pollen, such as *Cranwellia stiatella* and *Lythraidites debilis*, occurred at a ratio of

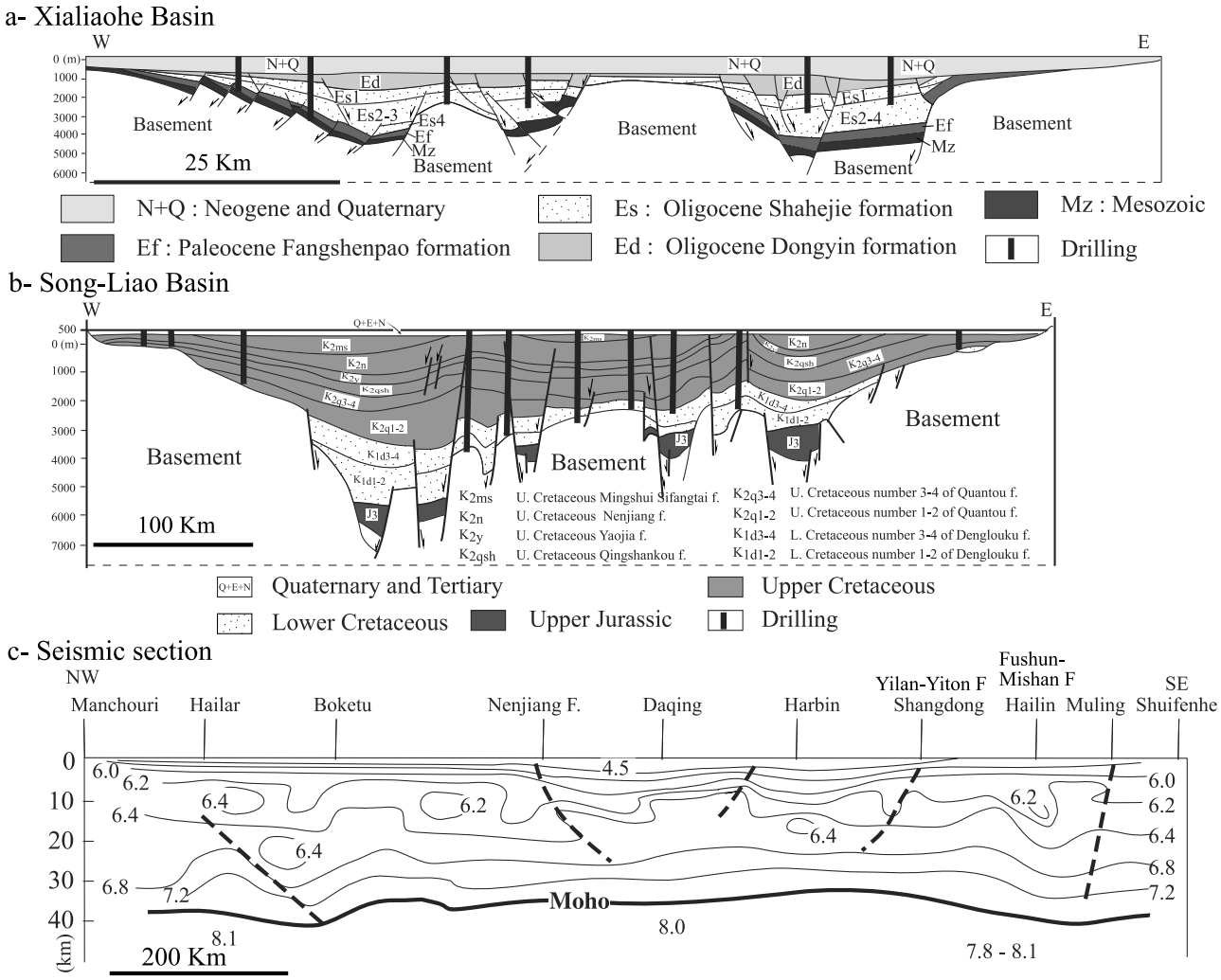

Figure 8. Cross sections through (a) the Xialiaohe basin and (b) the Songliao basin [*Chen et al.*, 1999]. (c) A structural reinterpretation of a seismic section at the crustal scale [after *Yu*, 1989]. All sections are located in Figure 1.

9–30% in the Quantou formation (K_2 [*Li*, 2001]). Therefore the age of the Quantou formation is confidently assigned to the Turonian and Cenomanian (Figure 9). Marine transgressions that occurred in the upper portion of the Qingshankou formation (K_2) and the lower portion of the Nenjiang formation (K_2) are evidenced by brackish to seawater fossils, glauconite, as well as calcareous nannofossils in condensed sections (Figure 9) [*Ye and Wei*, 1996]. The Latest Cretaceous Sifangtai and Mingshui formations composed of fluvial sediments are preserved only in the western part of the Songliao basin, in agreement with a westward migration of the depocenter at the end of Mesozoic time. The Oligocene deposited unconformably on slightly folded Cretaceous strata.

[27] Recent geochemical and geochronological studies of the volcanic rocks in the Songliao basin provided evidences for a subduction-related tectonic setting for a part of the Cretaceous magmatism [e.g., *Wang et al.*, 2002, and references therein]. Wang et al. relate this magmatism to a southward subduction along the Mongol-Okhostsk Belt (Figure 1). However, such an interpretation is not supported by geologic observations since the Mongol-Okhotsk Belt trends E-W along several hundred kilometers, whereas the Songliao volcanic rocks develop along a NNE-SSW trend, that is to say, nearly perpendicular to the Mongol-Okhotsk Belt to the inferred subduction zone. It is worth noting that a geochemical calc-alkaline signature of volcanic rocks does not preclude extensional tectonics. Indeed, in Cretaceous time the subduction zone along the eastern margin of Asia was located ~1000 km east of the Songliao basin. Therefore the development of the Sonliao basin can be considered as a rift basin mainly opened in Late Cretaceous-Cenozoic times within a Cretaceous magmatic arc.

[28] To the east of the Yilan-Yitong fault, the Sanjiang basin is a superimposed basin, in which Cretaceous lacustrine sediments are unconformably overlain by 3000-m-thick Tertiary dark colored mudstone [*Guo and Liu*, 1989]. In the Boli and Jixi basins (Figure 10a), only thick Cretaceous or Eocene sediments with thickness of 4000 m and 3000 m, respectively, are preserved.

[29] Regional seismic investigations show that the Songliao basin is characterized by a relatively thin con-

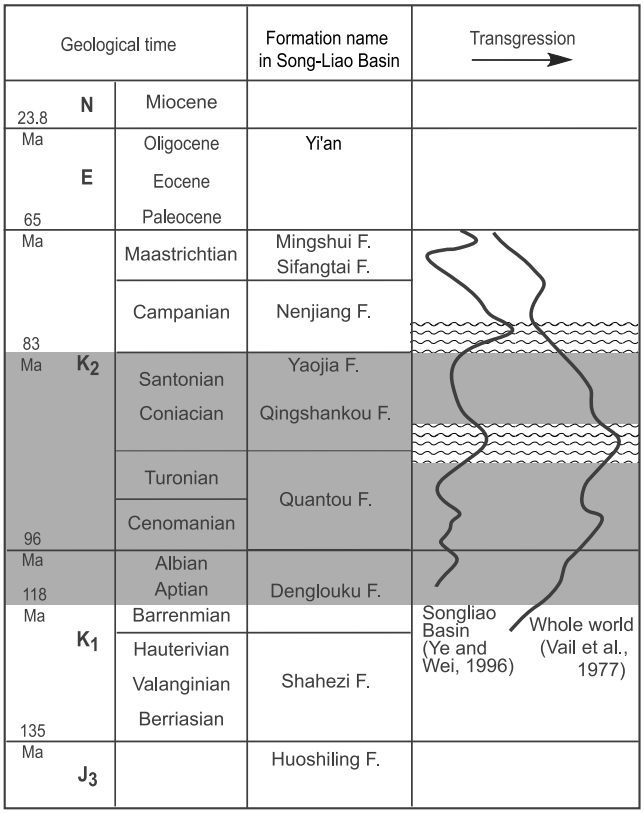

Figure 9. Comparison of the world transgression [after *Vail et al.*, 1977] to that of the Songliao basin [after *Ye and Wei*, 1996] characterizing the local basin evolution during the Late Cretaceous. The shaded zone presents the possible magnetic remanence age within the Cretaceous Long Normal Superchron (CLNS).

tinental crust and lithosphere with high heat flow [*Ma*, 1987; *Yu*, 1989; *Yang et al.*, 1997; *Menzies and Xu*, 1998]. The thickness of the crust varies from 29 to 35 km from the center to margin of the basin, respectively (Figure 8c) (In the Songliao basin surroundings, the crust reaches a 35–40 km thickness, and the lithosphere thickness ranges from 60 to 80 km, which is much thinner than those in the surrounding areas.) Thus geophysical observations suggest that the Songliao basin was developed in an extensional tectonic regime.

[30] The above mentioned evolution of the sedimentary basins in this region clearly reveals an inhomogeneous rifting history. In fact, all Late Jurassic to Early Cretaceous sediments in the region are coal measures, deposited in intramontane basins in west and south and paralic basins in northeast [*Li et al.*, 1983; *Bureau of Geology and Mineral Resources of Heilongjiang Province*, 1993]. The Late Cretaceous extension happened in an area much larger than the Songliao basin alone since the Xialiaohe basin in the south and the Sanjiang basin in the east also experienced the rifting event. The triangle-shaped rifting shows that this region experienced a differential extension from the north to the south. It seems clear that the extension is more important in the northern part than in the southern part. However, to the north, the extended area seems to be limited by the Mongol-Okhotsk suture, which has been reactivated as a left-lateral transfer fault in Late Cretaceous times [*Natal'in*, 1993]. In the south, the Xialiaohe basin stopped rifting in Early Cretaceous, although its activity became renewed again in the Eocene. Most of the Cretaceous strata have been eroded with only Lower Cretaceous rocks still preserved (Figure 8a). However, these emersion and erosion phenomena do not seem directly related to regional tectonics. As shown by the comparison between the sea level curves of the Songliao basin and the whole world (Figure 9), the Cretraceous erosion is likely related to global eustatic positive motions. The Songliao basin seems to end its extension at the end of the Cretaceous (Figure 8b). To the east of the Yilan-Yitong fault, the extension might stop also in the Cretaceous in the south, such as the Yanji basin (Figure 10a), and thick Eocene sediments developed only in its northern region (such as the Sanjiang basin). However, in the south of the NE China plain, the extension continuously lasted until at least to the Oligocene (Figure 8a), and coeval the sedimentary basin developed progressively from north to south.

[31] The heterogeneous rifting responsible for the rotation forms the triangle-shaped NE China plain may be related to the clockwise rotation of the ELK Block with respect to the Chinese Block. The ELK Block is separated from the NE China plain by the Fushun-Mishan fault (Figure 10a). In fact, the Fushun-Mishan fault is composed of two normal faults that make up a half graben basin. The normal fault on the west controls the sedimentary center of the Fushun basin (Figure 10a). The Neogene sediment in the basin is ~2000 m [*Wu et al.*, 2001], indicating that the main extension period is of Neogene. Similar to the Fushun-Mishan fault, the Yilan-Yitong fault system, situating at the east of Songliao basin, was also composed of two boundary faults that make up half grabens (Figure 10a). The west boundary fault is a growing fault facing to the east and controls the Neogene deposits of the graben. The sedimentary strata overlap to the east with maximum thickness >5000 m in the depocenter [*Liu et al.*, 1993].

[32] If taking into account 15 km for the difference between the initial and thinned crust thickness [*Kirillova*, 1995], the ~20° ± 10° clockwise rotation of the NE China plain centered nowadays in the south of the Bohai Bay (Figure 10b) would correspond to an extension amount of about 300 ± 150 km in the north part of the plain. This paleomagnetic estimation complies with the tectonic reconstructions showing that the present basin with of ~700 km results of the stretching of a segment with an initial width of ~500 km. In fact, this extension affected an area wider than 800 km in north (i.e., the Songliao basin plus the basins east of the Yilan-Yitong fault), whereas the width of the extended domain in the south (i.e., the Xialiaohe basin, Figure 8a) is <80 km. Geological data indicate that the rifting might begin before the early Late Cretaceous. In addition, sinistral strike-slip motion along the Yilan-Yitong fault and the Fushun-Mishan fault, as well as faults within the Songliao basin [*Li and Li*, 1999], might also have absorbed parts of the rotation. Therefore the proposed rotational rifting accounts for the amount of extension of the northern termination of the basins. The sedimentological study shows that the oldest sediments in the bottom of these basins are of Late Jurassic age, indicating that the rifting started at that time. Since a relatively important rate of

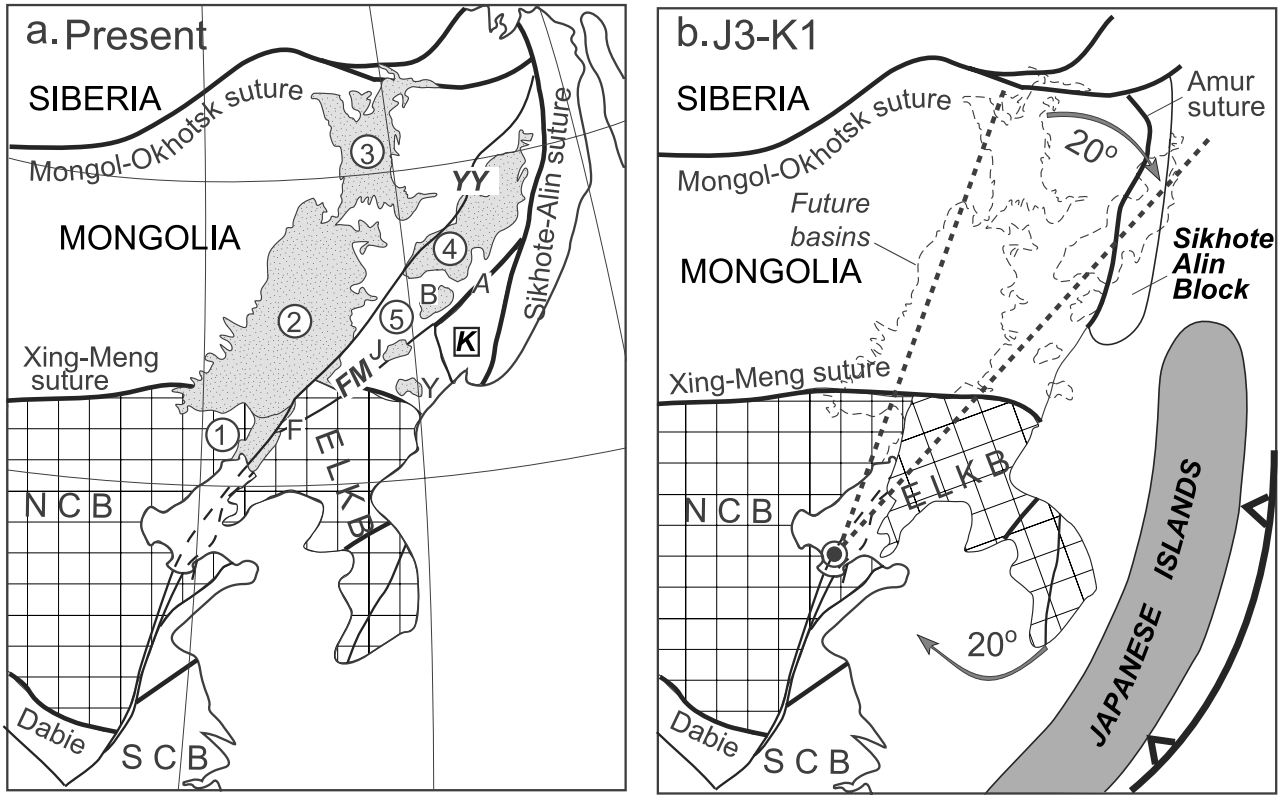

Figure 10. Reconstruction of the rotational rifting in NE China. (a) Present view of NE Asia. Basins are (numbered circles) 1, Xialiaohe basin; 2, Songliao basin; 3, Zeya basin; 4, Sanjiang basin; 5, relic basins east of Yilang-Yiton fault with B, Boli basin; J, Jixi basin; Y, Yanji basin. Faults are A, Amur suture; YY, Yilan-Yitong fault; FM, Fushun-Mishan fault. K in square indicates the Khanka massif. (b) A Jurassic-Cretaceous reconstruction by counterclockwise rotation of ~20°. The rotation pole is fixed in the southern termination of the Xialiaohe basin.

sedimentation is observed for the Late Jurassic-Early Cretaceous period (Figures 8a and 8b), it is reasonable to think that the ELK Block suffered a larger rotation since the Jurassic time. A tentative reconstruction of the eastern Eurasia margin in Late Jurassic-Early Cretaceous times taking into account the 20° clockwise rotation of the ELK Block and the coeval opening of the Songliao and other rift basins is proposed in Figure 10b. Some microcontinents such as Sikhote-Alin and Japanese islands are represented according to *Faure and Natal'in* [1992].

[33] One may argue that the Cenozoic basins in the south of Bohai, such as Jizhong and Subei basins, should be also considered in this kinematic model as they are probably be "coeval" and/or formed by the same geodynamic cause [e.g., *Allen et al.*, 1997, 1998]. Because of the structural complexity and the great width of the area involved in this large-scale tectonics, since the area ranges from 30 to 50°N and 114 to 130°E in latitude and longitude, respectively, the development of these basins is controlled by different (reactivated) structural systems. The seismic profiles from the Songliao and Xialiaohe basins show rather similar tectonic structures: the NNE-SSW oriented normal faults are parallel to major faults, such as the Tan-Lu, Yilan-Yiton, and Nenjian faults (Figure 8). It is not the case for the southern basins. For example, Bohai basin is essentially controlled by two groups of normal faults in NNE-SSW and ENE-WSW directions. The latter is almost orthogonal to the major structures. This basin has meanwhile experienced two styles of deformation: extensional and partial compressional in the northern and southern parts, respectively [*Qian and Han*, 2001]. These two different styles of deformation within the same basin have been also shown in other southern basins, such as the Subei basin: with extension in the south and compression in the north [*Chen et al.*, 2001]. As the analysis of deformation styles and kinematic history is beyond this study, we will not discuss them in detail here. Additional paleomagnetic studies in these areas may offer more opportunities to this debate.

[34] From the geodynamic point of view, several hypotheses may explain the clockwise rotation of the ELK Block. Basically, two kinds of models involve either asthenospheric or lithospheric layers. Mantle upwelling related to asthenospheric convection widely developed below east Asia has been proposed to account for the petrology and geochemistry of mantle xenoliths scavenged by Cenozoic volcanics [e.g., *Menzies and Xu*, 1998]. Other models consider NE China rifting to be linked to the subduction of the Pro-Pacific Ocean below the eastern margin of Eurasia [e.g., *Ren et al.*, 2002, and references therein]. In the present state of knowledge a detail discussion of these models is beyond the scope of this paper, which is restricted to the kinematic aspects. In order to provide stronger constraints on these models, more paleomagnetic, structural, geochemical, and geochronological surveys involving larger

temporal and spatial spans have to be carried out in near future.

5. Conclusions

[35] In Eastern Liaoning Province, Paleozoic and Late Permian-Early Triassic rocks are unfortunately remagnetized by the recent geomagnetic field; however, Late Cretaceous red tuffaceous sandstone passes the positive fold test, shows no PEF ChRM carried by both magnetite and hematite, presents a solo normal polarity, and thus provides the only reliable paleomagnetic data in this study. The good coherence between all available Cretaceous paleomagnetic data from Eastern Liaoning-Korean Peninsula indicates that this zone belongs to a single tectonic unit since that time, namely, the East Liaoning-Korea (ELK) Block. A significant difference in magnetic declination has been evidenced between the ELK Block and NCB plus SCB (the Chinese Block). This difference may be interpreted as a differential rotation (22.5° ± 10.2°) with a negligible latitudinal displacement (0.8° ± 6.1°) between these two tectonic units. This observation indicates that left-lateral displacement along the Tan-Lu fault, if there was any, should have occurred before the Late Cretaceous. Moreover, the Korean Block cannot be considered as a rigid part of NCB. A Meso-Cenozoic rifting model has been documented to illustrate this relative rotation. The triangle-shaped NE China plain has experienced heterogeneous rifting from the late Jurassic to the Oligocene-Miocene, forming several basins. Its larger extension in the north may be accommodated with a clockwise rotation of the ELK Block centered at the south of the present Bohai Bay. This model may be tested by more paleomagnetic constraints spanning from the NE China plain and Korea.

[36] **Acknowledgments.** The results presented in this study are outcoming from Chinese National 973 Project G1999043303, NSFC 40202021, JSPS (02060), and the Sino-French cooperating project PRA T01-03. Some of the measurements were carried out at the Institut de Physique du Globe de Paris (Jussieu and Saint Maur). The magnetic direction analyses were performed by Enkin's and Congé's computing programs. We thank also Christel Hatton and Tan Xiaodong for the laboratory assistance. We thank Carlo Laj, the Associate Editor, Boris Natal'in, and Mark Allen for their constructive reviews to improve the original manuscript.

References

Allen, M. B., D. I. Macdonald, X. Zhao, S. Vincent, and C. Brouet-Menzies, Early Cenozoic two-phase extension and late Cenozoic thermal subsidence and inversion of the Bohai Basin, Northern China, *Mar. Petrol. Geol.*, *14*, 951–972, 1997.

Allen, M. B., D. I. Macdonald, X. Zhao, S. Vincent, and C. Brouet-Menzies, Transtensionnal deformation in the evolution of the Bohai Basin, northern China, in *Continental Transpressional and Transtensional Tectonics*, edited by R. E. Holdsworth, R. A. Strachan, and J. Dewey, *Geol. Soc. Spec. Publ.*, *135*, 215–229, 1998.

Avouac, J.-P., and P. Tapponnier, Kinematic model of active deformation in central Asia, *Geophys. Res. Lett.*, *20*, 895–898, 1993.

Besse, J., and V. Courtillot, Revised and synthetic apparent polar wander paths of the African, Eurasian, North American and Indian plates, and true polar wander since 200 Ma, *J. Geophys. Res.*, *96*, 4029–4050, 1991.

Besse, J., and V. Courtillot, Apparent and true polar wander and the geometry of the geomagnetic field in the last 200 million years, *J. Geophys. Res.*, *107*(B11), 2300, doi:10.1029/2000JB000050, 2002.

Bureau of Geology and Mineral Exploration and Development of Liaoning Province (BGMEDLP), *Stratigraphy (Lithostratic) of Liaoning Province*, 247 pp., China Univ. of Geosci. Press, Beijing, 1997.

Bureau of Geology and Mineral Resources of Heilongjiang Province, *Regional Geology of Heilongjiang Province* (in Chinese with English abstract), 734 pp., Geol. Publ. House. Beijing, 1993.

Bureau of Geology and Mineral Resources of Liaoning Province (BGMRLP),, *Regional Geology of Liaoning Province* (in Chinese with English abstract), *Geol. Mem. Ser. 1*, 856 pp., Geol. Publ. House, Beijing, 1989.

Chan, L., Paleomagnetism of Late Mesozoic granitic intrusions in Hong Kong: Implications for upper Cretaceous reference pole of south China, *J. Geophys. Res.*, *96*, 327–335, 1991.

Chen, A., Geometric and kinematic evolution of basement-cored structure: Intraplate orogenesis within the Yanshan Orogen, north China, *Tectonophysics*, *292*, 17–42, 1998.

Chen, D., Y. Fan, and H. Zhao, Analysis on the genesis of Mesozoic volcanic formations in northeast China and adjacent area, *Geol. Resour.*, *10*(2), 66–70, 2001.

Chen, J., X. Cai, C. Lin, H. Wang, and M. Lei, Tectonic characteristics and episodic evolution of the northern fault depression in Songliao Basin (in Chinese with English abstract), *Acta Petrol. Sin.*, *20*(4), 14–18, 1999.

Chen, Y., H. Wu, V. Courtillot, and S. Gilder, Large N-S convergence at the northern edge of the Tibetan Plateau? New Early Cretaceous paleomagetic data from Hexi Corrido, NW Chinar, *Earth Planet. Sci. Lett.*, *201*, 293–307, 2002.

Cheng, Y. Q., (Ed.), Geological map of China, scale 1:5,000,000, Geol. Publ. House, Beijing, 1990.

Cong, B., (Ed.), *Ultrahigh-Pressure Metamorphic Rocks in the Dabieshan-Sulu Region of China*, 224 pp., Kluwer Acad., Norwell, Mass., 1996.

Doh, S., and J. Piper, Paleomagnetism of the (uper Paleozoic-Lower Mesozoic Pyongan Supergroup, Korea: A Phanozoic link with the North China Block, *Geophys. J. Int.*, *117*, 850–863, 1994.

Enkin, R. J., Y. Chen, V. Courtillot, J. Besse, L. Xing, Z. Zhang, Z. Zhuang, and J. Zhang, A Cretaceous pole from South China, and the Mesozoic hairpin turn of the Eurasian apparent polar wander path, *J. Geophys. Res.*, *96*, 4007–4027, 1991.

Enkin, R. J., Z. Yang, Y. Chen, and V. Courtillot, Paleomagnetic constraints on the geodynamic history of the major blocks of China from the Permian to the Present, *J. Geophys. Res.*, *97*, 13,953–13,989, 1992.

Faure, M., and B. Natal'in, The geodynamic evolution of the eastern Eurasian margin in Mesozoic times, *Tectonophysics*, *208*, 397–411, 1992.

Faure, M., W. Lin, L. Shu, Y. Sun, and U. Schärer, Tectonics of the Dabieshan (E. China) and possible exhumation mechanism of ultra high-pressure rocks, *Terra Nova*, *11*, 251–258, 1999.

Fisher, R., Dispersion on a sphere, *Proc. R. Soc. London, Ser. A*, *217*, 295–305, 1953.

Gilder, S., and V. Courtillot, Timing of the north-south China collision from new middle to late Mesozoic paleomagnetic data from the North China Block, *J. Geophys. Res.*, *102*, 17,713–17,727, 1997.

Gilder, S., R. Coe, H. Wu, X. Kuang, X. Zhao, Q. Wu, and Z. Tang, Creteceous and Tertiary paleomagnetic results from southeast China and their tectonic implications, *Earth Planet. Sci. lett.*, *131*, 637–652, 1993.

Gilder, S., P. Leloup, V. Courtillot, Y. Chen, R. Coe, X. Zhao, W. Xiao, N. Halim, J.-P. Cogné, and R. Zhu, Tectonic evolution of the Tancheng-Lujiang (Tan-Lu) fault via Middle Triassic to Early Cenozoic paleomagnetic data, *J. Geophys. Res.*, *104*, 15,365–15,390, 1999.

Guo, C., and J. Liu, Tectonics and prospects prediction of petroliferous area in northeast China, in *The Symposium on Structural Features of Oil and Gas Bearing Areas in China*, edited by Z. Tian et al., pp. 35–46, Pet. Ind. Press, Beijing, 1989.

Hsu, V., Paleomagnetic results from one of the red basins in south China (abstract), *Eos Trans. AGU*, *68*, 295, 1987.

Hu, L., P. Li, and X. Ma, A magnetostratigraphic study of Cretaceous red beds from Shanghang, western Fujian (in Chinese), *Geol. Fujian*, *1*, 33–42, 1990.

Huang, K., and N. Opdyke, Paleomagnetism of Cretaceous to mower Tertiary rocks from southwestern Sichuan: A revisit, *Earth Planet. Sci. Lett.*, *112*, 29–40, 1992.

Jahn, B. M., X. H. Zhou, and J. L. Li, Formation and tectonic evolution of southeastern China and Taiwan: Isotopic and geochemical constraints, *Tectonophysics*, *183*, 145–160, 1990.

Jelinek, V., Characterization of the magnetic fabric of rocks, *Tectonophysics*, *79*, 563–567, 1981.

Kent, D., X. Zeng, X. Zhang, and N. Opdyke, Widespread late Mesozoic to recent remagnetization of Paleozoic and Lower Triassic sedimentary rocks from South China, *Tectonophysics*, *139*, 133–143, 1987.

Kimura, G., M. Takarashi, and M. Kono, Mesozoic collision-extrusion tectonics in eastern Asia, *Tectonophysics*, *181*, 12–23, 1990.

Kirillova, G., A comparative study of intracontinental rift basins of East Asia: Songliao and Amur-Zeya, *Geol. Pac. Ocean*, *11*, 909–936, 1995.

Kirschvink, J. L., The least squares line and the analysis of paleoamgnetic data, *Geophys. J. R. Astron Soc.*, *62*, 699–718, 1980.

Lee, G., J. Besse, V. Courtillot, and R. Montigny, Eastern Asia in Cretaceous: New paleomagnetic data from South Korea and a new look at Chinese and Japanese data, *J. Geophys. Res.*, *92*, 3580–3596, 1987.

Li, J., and J. Li, Genetic types and accumulation modes of structural Albelt in the southeast uplift of Songliao Basin, *Pet. Geol. Oilfield Dev. Daqing*, *18*, 7–9, 1999.

Li, S., B. Li, Z. Li, and J. Huang, Evolution of Mesozoic and Cenozoic coal basins in the eastern China (in Chinese), in *Structure and Evolution of Mesozoic and Cenozoic Basins*, edited by X. Zhu, pp. 142–149, Science Press, Beijing, 1983.

Li, S., Y. Chen, B. Cong, Z. Zhang, R. Zhang, D. Liou, S. R. Hart, and N. Ge, Collision of the North China and Yangtze Blocks and formation of coesite-bearing eclogites: Timing and processes, *Chem. Geol.*, *109*, 70–89, 1993.

Li, W., Palynoflora from the Quantou formation of Songliao Basin, NE China and its bearing on the Upper/Lower Cretaceous boundary (in Chinese with English abstract), *Acta Palaeontol. Sin.*, *40*, 153–176, 2001.

Li, Z., Collision between the North and South China Blocks: A crust-detachment model for suturing in the region east of the Tan-Lu fault, *Geology*, *22*, 739–742, 1994.

Li, Z., I. Metcalfe, and X. Wang, Vertical-axis bock rotations in southwestern China since the Cretaceous: New paleomagnetic results from Hainan Island, *Geophys. Res. Lett.*, *22*, 3071–3074, 1995.

Liaoning Bureau of Geology and Mineral Resources-Kuandian, Geologic map of the Kuandian, scale 1:200,000, Minist. of Geol. and Miner. Resour., Beijing, 1967.

Lin, J., The apparent polar wander paths for the north and south China blocks, Ph.D. thesis, 248 pp., Univ. of Calif., Santa Barbara, 1985.

Lin, W., M. Faure, P. Monié, U. Schäerer, L. Zhang, and Y. Sun, Tectonics of SE China, new insights from the Lushan massif (Jiangxi Province), *Tectonics*, *19*, 852–871, 2000.

Liu, J., Cenzoic Volcano in northeastern China, *Acta Petrol. Sin.*, *41*, 1–10, 1988.

Liu, M., B. Yang, and J. Deng, *The Geological Structure Feature of Yilan-Yitong Graben and Its Evolution*, 258 pp., Geol. Publ. House, Beijing, 1993.

Ma, X. Y., Lithospheric dynamics map of China and adjacent seas (1:4,000,000) and exploratory notes (in Chinese), map, Geol. Publ. House, Beijing, 1987.

Ma, X., Z. Yang, and L. Xing, The Lower Cretaceous reference pole from the North China and its tectonic implications, *Geophys. J. Int.*, *115*, 323–331, 1993.

Mattauer, M., P. Matte, J. Malavieille, P. Tapponnier, H. Maluski, Z. Xu, Y. Lu, and Y. Tang, Tectonics of Qinling belt: Build-up and evolution of eastern Asia, *Nature*, *317*, 496–500, 1985.

Menzies, M., and Y. Xu, Geodynamics of the North China Craton, in *Mantle Dynamics and Plate Interactions in East Asia*, *Geodyn Ser.*, vol. 27, edited by F. Martin et al., pp. 151–165, AGU, Washington, D. C., 1998.

Nata'in, B., History and modes of Mesozoic accretion in southeastern Russia, *Island Arc*, *2*, 15–34, 1993.

Odin, G., Geological time scale, *C. R. Acad. Sci.*, *318*, 59–71, 1994.

Okay, A., A. Sengor, and M. Satir, Tectonics of an ultrahigh-pressure metamorphic terrane: The Dabieshan/Tongbaishan orogen, China, *Tectonics*, *12*, 1320–1334, 1993.

Otofuji, Y., K. Kim, H. Inokuchi, H. Morinaga, F. Murata, and H. Y. K. Katao, A paleomagnetic reconnaissance of Permian to Cretaceous sedimentary rocks in southern part of Korean Peninsula, *J. Geomagn. Geoelectr.*, *38*, 387–402, 1986.

Otofuji, Y., Y. Liu, M. Yokoyama, M. Tamia, and J. Yin, Tectonic deformation of the southwestern part of the Yangtze craton inferred from paleomagnetism, *Earth Planet. Sci. lett.*, *156*, 47–60, 1998.

Peltzer, G., P. Tapponnier, Z. Zhang, and Z. Xu, Neogene and Quaternary faulting in and along the Qinling Shan, *Nature*, *317*, 500–505, 1985.

Pruner, P., Paleomagnetism and paleogeography of Mongolia from the Carboniferous to Cretaceous-Final report, *Phys. Earth Planet. Inter.*, *70*, 169–177, 1992.

Qian, J., and Z. Han, A comparison study on the exploration potential between Bohai Bay basin and Subei Basin, *Pet. Explor. Dev.*, *28*, 15–18, 2001.

Ratsbacher, L., B. Hacker, L. Webb, M. McWilliams, T. Ireland, S. Dong, A. Calvert, D. Chateigner, and H.-R. Wenk, Exhumation of ultrahigh-pressure continental crust in east central China: Cretaceous and Cenozoic unroofing and the Tan-Lu fault, *J. Geophys. Res.*, *105*, 13,303–13,338, 2000.

Ren, J., K. Tamaki, S. Li, and J. Zhang, Late Mesozoic and cenozoic rifting and its dynamic setting in Eastern China and adjacent areas, *Tectonophysics*, *344*, 175–205, 2002.

Sun, S., J. Li, J. Lin, Q. Wang, and H. Chen, Indosinides in China and the consumption of eastern paleotethys, in *Controversies in Mordern Geology*, edited by D. W. Muller, J. A. McKenzie, and H. Weissert, pp. 363–384, Academic, San Diego, Calif., 1991.

Tarling, D., and F. Hrouda, *The Magnetic Anisotropy of Rocks*, Chapman and Hall, New York, 1993.

Uchimura, H., M. Kono, H. Tsunawaka, G. Kimura, Q. Wei, T. Hao, and H. Liu, Palaeomagnetism of late Mesozoic rocks from northeastern Chin: The role of the Tan-Li fault in the North China Block, *Tectonophysics*, *262*, 301–319, 1996.

Uno, K., Clockwise rotation of the Korean Peninsula with respect to the North China Block inferred from an improved Early Triassic palaeomagnetic pole for the Ryeongnam Block, *Geophys. J. Int.*, *143*, 969–976, 2000.

Vail, P. R., R. M. Mitchum Jr., and S. Thompson, Seismic stratigraphy and global changes of sea level, part four: Global cycles of relative changes of sea level, *AAPG Mem.*, *26*, 83–98, 1977.

Wang, P., W. Liu, S. Wang, and W. Song, $^{40}Ar/^{39}Ar$ and K/Ar dating on the volcanic rocks in the Songliao basin, NE China: Constraints on stratigraphy and basin dynamics, *Int. J. Earth Sci.*, *91*, 331–340, 2002.

Watson, G., and R. Enkin, The fold test in paleomagnetism as a parameter estimation problem, *Geophys. Res. Lett.*, *20*, 2135–2137, 1993.

Wu, C., X. Wang, G. Liu, S. Li, X. Mao, and X. Li, Tectonic evolution in Fushun Basin and its geodynamic research, *Sci. China*, *316*, 477–485, 2001.

Wu, H., L. Zhou, Z. Zhao, Z. Yang, and Y. Chen, Paleomagnetic results of the late Paleozoic and Mesozoic from the Alashan area of the northwestern China Block, *Sci. Geol. Sin.*, *2*, 19–46, 1993.

Xu, J., and G. Zhu, Tectonic models of the Tan-Lu fault zone, eastern China, *Int. Geol. Rev.*, *36*, 771–784, 1994.

Xu, J., G. Zhu, W. Tong, K. Cui, and Q. Liu, Formation and evolution of the Tancheng-Lujiang wrench fault system: A major shear system to the northwest of the Pacific Ocean, *Tectonophysics*, *134*, 273–310, 1987.

Xu, S., Y. Liu, L. Jiang, W. Su, and S. Ji, *Tectonic Regime and Evolution of Dabie Mountains* (in Chinese with English abstract), 175 pp., Science Press, Beijing, 1994.

Yang, B., S. Mu, X. Jin, and C. Liu, Comprehensive geology study in the Manzhouli-Suifenhe geoscience transcet, China, *Chin. J. Geophys.*, *40*, 27–40, 1997.

Yang, Z., and J. Besse, New Mesozoic apparent polar wander path for south China: Tectonic consequence, *J. Geophys. Res.*, *106*, 8493–8520, 2001.

Ye, S., and K. Wei, Condensed section and new evidence of marine inundation in Cretaceous, Songliao Basin, *Earth Sci. J. China Univ. Geosci.*, *21*, 267–271, 1996.

Yin, A., and S. Nie, An indentation model for the north and south China collision and the development of the Tan-Lu and Honam fault systems, eastern Asia, *Tectonics*, *12*, 801–813, 1993.

Yu, T., Structural features for hydrocarbon distribution in Lower Liaohe fault depression, in *The Symposium on Structural Features of Oil and Gas Bearing areas in China*, edited by Z. Tian et al., pp. 79–92, Pet. Ind. Press, Beijing, 1989.

Zhai, Y., M. Seguin, Y. Zhou, J. Deng, and Y. Zheng, New paleoamgnetic data from the Huanan block, China and Cretaceous tectonics in eastern China, *Phys. Earth Planet. Inter.*, *73*, 163–188, 1993.

Zhao, X., and R. Coe, Paleomagnetic constraints on the collision and rotation of north and south China, *Nature*, *327*, 141–144, 1987.

Zhao, X., R. S. Coe, Y. Zhou, H. Wu, and J. Wang, New paleomagnetic results from nothern China: Collision and suturing with Siberia and Kazakhstan, *Tectonophysics*, *181*, 43–81, 1990.

Zhao, X., R. Coe, K. Chang, S. Park, S. Omarzai, R. Zhu, Y. Zhu, S. Gilder, and Z. Zheng, Clockwise rotations recorded in Early Creataceous rocks of South Korea: Implications for tectonic affinity between the Korean Peninsula and north China, *Geophys. J. Int.*, *138*, 447–463, 1999.

Zheng, S., and W. Zhang, General description of Mesozoic plant family of Liaoning, *J. Geol. Liaoning*, *1*, 14–17, 1981.

Zheng, Z., M. Kono, H. Tsunakawa, G. Kimura, Q. Wei, X. Zhu, and T. Hao, The apparent polar wander path for the North China Block since the Jurassic, *Geophys. J. Int.*, *104*, 29–40, 1991.

Zhu, Z., T. Hao, and H. Zhao, Paleomagnetic study on the tectonic motion of the Pan-Xi block and adjacent area during Yinzhi-Yanshan period, *Acta Geosci. Sin.*, *31*, 420–431, 1988.

Y. Chen and M. Faure, Département des Sciences de la Terre, ISTO, Université d'Orléans, F-45067 Orléans cedex 02, France. (Yan.Chen@univ-orleans.fr)

W. Lin, Department of Earth and Planetary Sciences, Nagoya University, Chikusa, Nagoya 464-8602, Japan.

Q. Wang, Institute of Geology and Geophysics, Chinese Academy of Sciences, 100029, Beijing, China.